Klinik für Traumatologie
des Universitätsspitals Zürich

Direktor: Prof. Dr. med. Hans-Christoph Pape

Analysis of Human Adipose-derived Stem Cell Subpopulations by Mass Cytometry for Osteogenic Differentiation

Inaugural-Dissertation

zur Erlangung der Doktorwürde der
Vetsuisse-Fakultät Universität Zürich

vorgelegt von

Anna Mirjam Eichrodt

Tierärztin
von Basel BS

genehmigt auf Antrag von

PD Dr. Paolo Cinelli, Referent

PD Dr. Raffaella Santoro, Korreferentin

2019

Contents

Abstract

Treatments of critical size bone defects represent a clinical challenge. Gold standard therapy includes autogenous bone graft and alloplastic materials. However, restricted graft availability, pain, and morbidity limit this therapy. A promising alternative presents tissue engineering with mesenchymal stem cells derived from the adipose tissue, the so-called adipose-derived stem cells (ASCs). These cells can be obtained easily and in high numbers. Nevertheless, ASCs consist of a heterogeneous population of cells. Hence, it is likely that specific subpopulations with a higher propensity for osteogenic differentiation exist. This Doctoral Thesis dissects the heterogeneity within human ASCs to identify subpopulations more prone to osteogenic differentiation. We performed *in vitro* osteogenic differentiation using ASCs derived from 20 patients. Alizarin red staining and RTQ-PCR showed considerable differences. The CyTOF technology allowed analysis on cell by cell level. We found that the ASC lines from different patients contained several subpopulations, one of them was identified to be more abundant in good osteogenic differentiating lines.

In conclusion, differences between the ASC lines were verified and correlate with the clinical outcomes observed. Thus, identification of the subpopulation with high osteogenic potential could improve therapy of fractures and predict clinical outcomes.

Zusammenfassung

Die Behandlung von Knochendefekten kritischer Grösse stellt eine klinische Herausforderung dar. Die Goldstandardtherapie umfasst autogenes Knochentransplantat kombiniert mit alloplastischen Materialien. Nachteile dieser Therapie sind eingeschränkte Verfügbarkeit des Transplants, Schmerzen und Morbidität. Ein vielversprechender Ansatz stellt das Tissue Engineering mit mesenchymalen, adipösen Stammstellen (ASCs) dar. Letztere sind leicht und in grosser Menge gewinnbar. ASCs sind jedoch sehr heterogen, daher ist anzunehmen, dass sie aus mehreren Subpopulationen zusammengesetzt sind. Diese Dissertation analysiert die Heterogenität menschlicher ASCs mit dem Ziel, spezifische Subpopulationen mit hohem Potenzial zur Knochendifferenzierung zu identifizieren. Wir führten eine *in vitro* osteogene Differenzierung mit ASCs von 20 Patienten durch. Alizarin Färungen und RTQ-PCR zeigten erhebliche Unterschiede zwischen den Patienten. CyTOF ermöglichte eine Analyse auf Einzellzellebene, wodurch bestätigt wurde, dass ASCs aus mehreren Subpopulationen bestanden. Eine spezifische Subpopulation wurde häufiger in Patienten mit guter Knochenheilung identifiziert.

Zusammengefasst konnten Unterschiede zwischen ASCs verschiedener Patienten verifiziert und mit den verschiedenen Heilungsverläufen korreliert werden. Eine Identifizierung der Subpopulation mit starkem Knochendifferenzierungspotential könnte die Therapie von Frakturen verbessern und klinische Verläufe vorhersagen.

Abbreviations

AP	alkaline phosphatase
AML	acute myeloid leukaemia
ASCs	adipose-derived mesenchymal stem cells
BMSCs	bone marrow stem cells
CD	clusters of differentiation
CSB	cell staining buffer
CyTOF	cytometry by time-of-flight
ddH_2O	distilled water
DMEM	Dulbecco's modified eagle medium
DMSO	dimethyl sulfoxide
ESCs	embryonic stem cells
FACS	fluorescence-activated cell sorting
FCS	fetal calf serum
FlowSOM	flow cytometry data analysis using self-organizing maps
HLA-DR	human leucocyte-DR
hMSCs	human mesenchymal stem cells
ICP	isotope-conjugated probes
IL	interleukin
iPSCS	induced pluripotent stem cells
ISCT	International Society for Cellular Therapy
MSCs	mesenchymal stem cells
PBS	phosphate-buffered saline
PCA	principal component analysis
PLGA	poly-lactic-co-glycolic acid
RF	radiofrequency
RT	room temperature
RTQ-PCR	real-time quantitative PCR
SPADE	spanning-tree progression of density-normalized events
SVF	stromal vascular fraction
t-SNE	t-stochastic neighbour embedding
TNF-α	tumour recrosis factor-alpha
VEGF	vascular endothelial growth factor

1 Introduction

1.1 Bone characteristics

Bone is a highly specialized tissue forming the fundamental framework of the human body. Osseous tissue not only has the function of mechanical support, but it is also responsible for several biological functions and possesses the unique characteristic of self-healing [1]. Through its hardness and rigidity, bone protects vital organs and also provides onsets for muscles enabling movements [2]. Bones take part in biological processes such as hematopoietic cell formation in the bone marrow, mineral homeostasis, and provide a reservoir for growth factors and cytokines [1, 3]. Furthermore, bone constantly undergoes remodelling in order preserve strength by replacing old bone and also to adjust to changing biomechanical forces such as overloading, growth, disuse or the time after a fracture's repair. The remodelling process is regulated through cytokines, hormones, and chemokines [1, 2].

As already mentioned, bone has the extraordinary property to fully regenerate without scarring. Nevertheless, in some cases bone healing disorders may occur. Reasons for failure of fracture-healing include large bone defects, pathological fractures, or negative influences such as insufficient blood supply, systemic diseases, or infection. All these reasons can lead to delayed- or even non-union of a fracture's site [4]. Skeletal defects occur following diseases, trauma, congenital anomalies, cancer resection, or hereditary defects. The treatment and repair of such defects, especially the so called "critical size bone defects", where bone loss is so gravely that it does not heal over time, represent a serious clinical challenge for re-constructive and orthopaedic surgery [5, 6]. Current treatments include bone substitutes from autogenous, xenogeneic as well as prosthetic materials. The gold standard approach for large bone reconstruction is considered to be autogenous bone grafts in combination with alloplastic materials. Normally, bone graft is obtained out of the iliac crest's spongiosa [4, 5]. However, the supply of autogenous bone graft is restricted due to limited availability, morbidity, and severe donor site pain. In contrast to autogenous bone grafts, allografts and xenografts bear the risks of infection, immune rejection, bone resorption, disease transmission, and diminished graft incorporation. Besides, these kind of grafts lack of osteogenic properties. What is more, xenogeneic substitutes have the risk of transfer of zoonotic diseases [5, 6]. To this end, also inorganic and alloplastic materials, for example ceramics or hydroxy-apatite, can serve as bone substitutes. Disadvantages like contour irregularities, infection, and structural failure can come along using these materials [6].

In general, no synthetic or natural material provides yet all the needs for bone regeneration but the patient's own bone. As the latter has restricted availability, improved therapeutic approaches are urgently needed [7]. The novel approach of tissue engineering raises a promising alternative as it would avoid current drawbacks in the treatments of critical size bone defects. Recently, a cellular-based approach was investigated by combining scaffolds with mesenchymal stem cells (MSCs) in order to achieve better healing in bone fractures [5].

1.2 Mesenchymal stem cells

Mesenchymal stem cells are defined by their occurrence in adult tissue, their specific surface antigen expression, and their multipotency [8, 9]. Human MSCs (hMSCs) were originally isolated from bone marrow [10]. In the meantime, hMSCs are being isolated not only from a variety of adult tissues, for example adipose tissue [11] or synovial fluid [12], but also from foetal tissue like the Wharton's jelly [8]. Moreover, MSCs show expression of a specific pattern of surface markers. To be able to identify MSCs, the International Society for Cellular Therapy (ISCT) has specified three minimal criteria [9]:

1. Plastic adherence when maintained in standard cell culture.
2. Expression of specific clusters of differentiation (CDs): positive for CD105, CD73, and CD90 but no expression for CD45, CD34, CD14 or CD11b, CD79 or CD19, and human leucocyte-DR (HLA-DR).
3. MSCs must be able to differentiate into osteoblasts, adipocytes, and chondroblasts.

Based on the first criterion, as an example, MSCs can be separated from freshly isolated cells of fat tissue, the so called stromal vascular fraction [13]. Another feature of MSCs represents their multipotency, enabling differentiation into the mesodermal cell lineages such as osteoblasts [14], chondrocytes [15], and adipocytes [16]. By now, not only differentiation into mesodermal tissue lineages, but also the capacity of differentiation into ectodermal tissue (for example skin, [17]) and endodermal tissue (for instance neural cells [18]) has been reported. Overall, MSCs are of great interest for cell therapy, regenerative medicine, and tissue repair. In contrast to embryonic stem cells (ESCs) and induced pluripotent stem cells (iPSCs), MSCs are effortlessly accessible, expandable *in vitro*, show exceptional genomic stability and present negligible ethical issues. Furthermore, MSCs are capable of multilineage potential, influence secretion of anti-inflammatory molecules and play a role in immunomodulation. These reasons are auspicious for treatment methods of chronic diseases. To sum up, MSCs are of paramount interest for clinical research. Recently, tissue engineering with MSCs has been studied using natural and synthetic biomaterials carrying stem cells as a therapeutic approach. Especially in orthopaedics, this strategy might lead to a significant improvement of current treatments. Not only the possibility of obtaining MSCs from various weaves, but also the use of a patients' very own cells declines the risk of immune-rejection [19].

Adipose-derived mesenchymal stem cells (ASCs) in particular represent an auspicious source for application in regenerative medicine. ASCs can be easily gained by lipoaspiration, a minimally invasive surgical technique providing a satisfactory quantity of cells [20]. Through their high proliferative rate, ASCs can subsequently be long-term expanded *in vitro*. Apart from their straightforward handling in cell culture, ASCs possess a great differentiation potential and a good genetic stability. On the other hand, stem cells obtained from the bone marrow (BMSCs) are used as a standard in research and in the clinical setting so far. These cells, however, have

many disadvantages, such as cell extraction which can only be performed by an invasive, quite painful procedure connected to a high risk of infection [21]. Furthermore, the isolated MSCs are more numerous in the adipose tissue than in the bone marrow [22]. Overall, ASCs show great potential for regenerative medicine due to their easy access by a low-risk procedure, their large amount of collected cells, and their effortless maintenance in cell culture.

MSCs consist of a heterogeneous mixture of different cells, which is mirrored in their protein expression, morphology, and differentiation potentials [23]. Despite this fact, all these cells meet the above-mentioned criteria of the ISCT [9]. Multiple studies reported single-cell derived colonies obtained from human MSCs enclose at least three different morphologies of stem and progenitor cells (reviewed in [23, 24]). Besides, not only numerous proteins are expressed on varying levels, but it is also suggested that specific stem cell subpopulations possessing a determined differentiation lineage subsist within a population of MSCs [23].

For instance, in one study ASCs were obtained from thirty humans and were then differentiated into endothelial cells and osteoblasts [25]. All cells had the ability to differentiate into those two lineages but were differently successful suggesting the existence of unalike cell populations among the donors. From these observations, it follows that extracting a particular subpopulation of ASCs more capable of differentiating towards a tissue of interest presents a favourable approach for regenerative medicine. Therefore, it is fundamental to further subdivide MSCs/ASCs and analyse more closely their differentiation potential [23]. What is more, multiple studies have reported that in general MSCs obtained from various sources express a great variety of markers (Tab. 1, [23]). For example, CD146 was positively expressed in BMSCs ([26, 27]), but was negative in hASCs [19]. Also, CD271 was found in ASCs but its expression lacked in other studies [19]. Another example is STRO-1, which was found in BMSCs but not in hASCs [28]. Clearly, a great variety of markers is found in literature (Tab. 1), and therefore, no exhaustive list can be proposed. Dissecting the heterogeneity of MSCs is essential for stem cell based methodologies as well as for better comprehension of biological behaviors [23]. In order to investigate this objective, the innovative technology of cytometry by time-of-flight offered a suitable approach.

1.3 Mass cytometry

Cytometry by time-of-flight (CyTOF), also known as mass cytometry, is an innovative breakthrough capable of real-time analysis of individual cells. Up to now, flow cytometry fluorescence-activated cell soring (FACS) was commonly used for single cell measurements for scientific purposes. With this method, cells previously stained with fluorescent-tagged antibodies are guided one at a time through laser beams consisting of different wavelengths. The fluorescent light of each cell is then converted into an electrical signal allowing profiling of subpopulations due to their expression and also quantification of their signals. However, as the spectral overlap of the fluorophores limits the amount of parameters that can be analysed simultaneously, FACS can only be operated with up to 18 protein markers. Cytometry by time-of-flight on the other

Table 1: Selected markers for mesenchymal stem cells.

Markers	Synonyms	Function	Cellular expression	Papers
MSC positive markers (from the ISCT)				
CD105	Endoglin	Angiogenesis; Modulation of cellular response to TGF beta 1	MSCs, endothelial cells, erythroid precursors, activated monocytes and makrophages	[9]
CD90	Thymocyte differentiation antigen 1 (THY1)	Costimulation of lymphocytes; cell adhesion	MSCs, hematopoietic cells, neuronal cells, fibroblasts, stromal cells, activated endothelial cells	[9]
CD73	5-nucleotidase, NT5E	An ecto-5-prime-nucleotidase hydrolyzing extracellular nucleotides into membrane permeable nucleosides	MSCs, T- and B-cell subsets, epithelial and endothelial cells, dendritic reticulum cells	[9]
MSC negative markers (defined from the ISCT)				
CD45	Lymphocyte common antigen	Regulation of T- and B-cell antigen receptor signaling; regulation of cell growth and differentiation	Hematopoietic cells (not platelets and erythrocytes)	[9]
CD14	LPS-Receptor	Receptor for LPS and LBP	Monocytes, macrophages, Langerhans cells, granulocytes	[9]
CD19	B-lymphocyte surface antigen B4, T-cell surface antigen Leu-12	Regulation of B-cell development, activation and differentiation; signal transduction	Hematopoietic cells (not platelets and erythrocytes)	[9]
CD11b	Integrin alpha M, CR3A, ITGAM	Cell adhesion; apoptosis; chemotaxis	Granulocytes, monocytes, natural killer cells, T- and B-cells, dendritic cells	[9]
Other markers				
NG2	Neuron-glial antigen 2	Pericyte marker expressed on the surface of MSCs	Neural progenitors, MSCs	[27]
CD146	MCAM, S-Endo1, A32 antigen, MUC18	Pericyte marker , intracellular adhesion, promotes tumor progression in many cancers	Endothelial cells, follicular dendritic cells, activated T-cells, smooth muscle, MSCs	[27, 26]
CD106	VCAM1, L1CAM	Adhesion of leukocytes; transmigration and costimulation of T-cells	Activated endothelial cells and follicular dendritic cells	[30]
STRO-1	-	Cell membrane proteine, which translocates due to intracellular calcium depletion	MSCs, endothelial cells	[31, 32]
CD271	Nerve growth factor receptor, p75NTR	Regulation of neuronal development (growth, migration, differentiation, apoptosis)	Schwann cells, neurons, bone marrow-derived MSCs	[33]
EGFR	Epidermal growth factor receptor	Tyrosine kinase receptor	Epithelial cells	[34]
PDGFRα	Platelet-derived growth factor receptor, alpha polypeptide	Tyrosine kinase receptor		[35]
CD38	ADP ribosyl cyclase 1	Regulation of cell activation; proliferation and adhesion	Variable expression on most hematopoietic and some non-hematopoietic cells. High expression: plasma cells, early T- and B-cells, natural killer cells, microglial cells	[36]
CD44	Epican, HUTCH-I, LHR, PGP-1, ECMR-III	Regulation of leukocytes (rolling, homing, aggregation, adhesion to endothelial cells, stromal cells, and extracellular matrix)	Most lympho-hematopoietic cells	[30]

hand evades the limitation of spectral overlap using stable heavy metal isotopes instead of fluorophores. This technique combines classical flow cytometry with mass spectrometry. CyTOF enables profiling of currently up to 40 surface markers at the same time on a per cell basis. Even more, mass cytometry has theoretically over 120 detection channels available which in future can be used as more isotopes become accessible. Mass cytometry enables profiling of function and phenotype in both, cells of healthy and diseased condition. So far, this technique has found application in research of immunology, oncology, haematology and drug development [29].

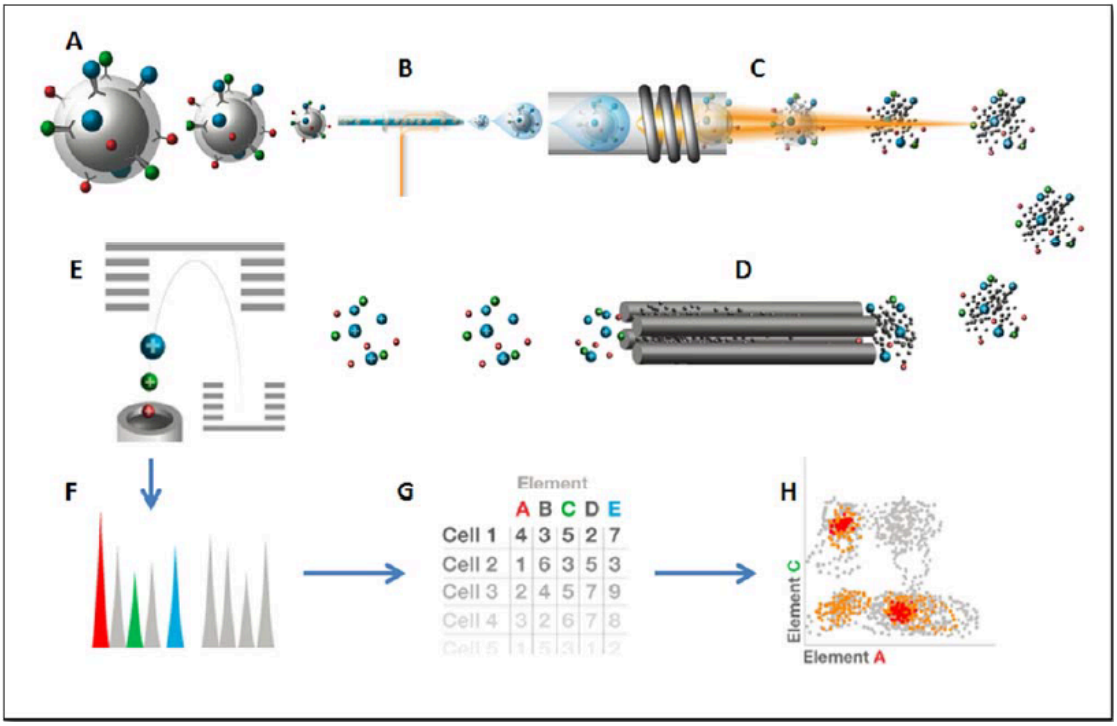

Figure 1: Cytometry by time-of flight workflow. *A* Cells stained with elemental isotope-labelled probes (ICPs) enter the nebulizer *B*, where the sample becomes aerosolized. The resulting aerosol droplets are introduced into the *C* ICP torch where they become vaporized, atomized and ionized. The radiofrequency (RF) quadrupole ion guide *D* removes low-mass ions. In the time-of-flight chamber (TOF, *E*), ions are separated according to their mass to charge ratio resulting in a mass spectrum *F* identifying and quantifying each isotope on single cell basis *G*. *H* The data can now be further analysed [29].

The first step in the mass cytometry workflow is the staining of the cells with elemental-isotope-labelled antibodies (Fig. 1). This liquid sample is directed into the nebulizer, where it becomes desolvated into single-cell aerosol droplets. These are then introduced into the isotope-conjugated probes (ICP) torch for vaporization, atomization and ionization. Next, the radiofrequency (RF) quadrupole ion guide removes low-mass ions in order to achieve an ion cloud enriched for the probe isotopes. Entering the time-of-flight (TOF) chamber, the ion cloud is accelerated towards a time-resolved detector separating the ions according to their mass to charge ratio.

Hence, the generated mass spectrum represents the quantity and identity of each isotope on a single cell basis. In the end, the produced .fcs files are available for data analysis, for example on a cloud-based platform named Cytobank [29].

For the analysis of the high dimensional data produced by a CyTOF machine, pre-processing is required, which includes data transformation, normalization, debarcoding, and gating. After these first steps, the data is visualized making use of clustering based methods or dimensionality reduction algorithms. The latter involves Principal Component Analysis (PCA) as well as T-Stochastic Neighbour Embedding (t-SNE) algorithms. PCA is based on the presumption that the relationship between the analysed parameters is linear. Thus, it calculates a smaller amount of parameters preserving the variability of the original data [37]. t-SNE in contrast consists of a non-linear approach visualizing similarities of cells on the basis of their marker expression in a two- or three-dimensional scatter plot. Related cells are situated closer to each other than unrelated cells enabling identification and characterization of smaller subpopulations [29]. Further to dimensionality reduction techniques, clustering based method can be applied for a visualization of mass cytometry data. Spanning-tree Progression of Density-Normalized Events (SPADE), for example, visualizes characteristics of cell subsets in a coloured hierarchical tree. However, this algorithm is not able to preserve single-cell resolution [37]. A second approach for clustering provides FlowSOM, an algorithm based on a self-organizing map providing several visualization options like tree structures or star charts [38]. A third algorithm called Citrus generates a dataset including all data from different samples, out of which cell populations can be determined by hierarchical clustering of phenotypically similar cells [37]. This means rephrased that Citrus identifies stratifying subpopulations. Another approach to analyse mass cytometry data is cell development modelling. Wanderlust and Phenograph are algorithms to analyze cellular differentiation processes [37].

A recently developed approach presents CellCnn, which allows detecting rare cell populations by representation learning [39]. CellCnn is able to determine rare cell subsets associated with a prior known phenotype (for instance healthy or diseased condition) from high dimensional measurements on a single cell basis. In order to achieve an association between the input of single cell measurements and the known phenotype the algorithm makes use of a convolutional neural network (Fig. 2). This network learns to represent a subpopulation through molecular profiles (filters) of single cells in terms of their frequency or presence. The single cells are associated with a phenotype [39] (Fig. 2). With this novel algorithm, for example, rare natural-killer-cell-subpopulations affiliated with cytomegalovirus infection have been identified [39].

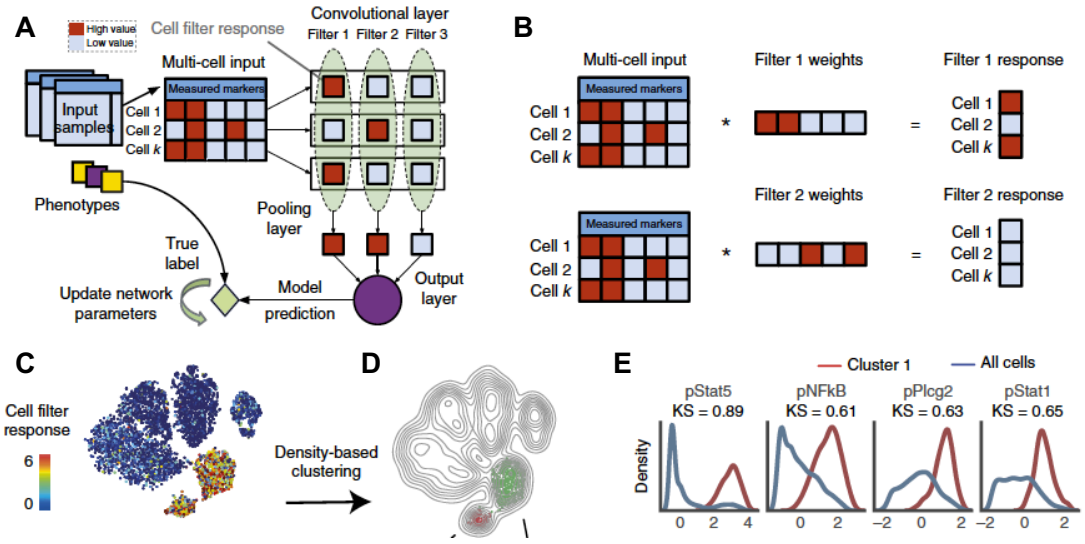

Figure 2: Illustration of CellCnn [39]. *A* Architecture of the convolutional neural network. CellCnn takes inputs of individual-cell measurements, which are assigned to a group connected with a phenotype. In the convolutional layer, node activities are defined as weighted sums over molecular profiles of individual cells. In the pooling layer the frequency (= mean pooling) or the presence (= max pooling) of particular cell subsets are estimated. The output layer of the neural network evaluates the phenotype. Network training improves weights to correspond to molecular profiles of significant cell subpopulations allowing annotating individual cells to a cell subset (cell-filter response). *B* Cell-filter response for single cells. For example, marker profile of cell one matches with filter 1 and therefore results in a high (red) cell-filter response (low filter response = grey). *C* t-SNE projection coloured based on the cell filter response of individual cells allowing to distinguish density based clusters *D*. *E* Greatest differential abundance between the whole cell-population and the chosen cell subpopulations using the Kolmogorov-Smirnov two-sample test [39].

1.4 Aims of Doctoral Thesis

Using MSCs in regenerative medicine for therapeutic applications in orthopaedics is a highly promising approach. In particular, adipose tissue has been determined as an excellent source of multipotent mesenchymal stem cells. These cells can be potentially used for improving fracture healing in critical size bone defects. However, ASCs consist of a heterogeneous cell population covering dissimilar stem and progenitor cells of variable differentiation potentials. For this reason, it is of paramount importance to identify cell subsets more prone to osteogenic differentiation potentials to realize better bone regeneration in defects, especially in critical size bone defects. The aim of this Doctoral Thesis is to scrutinize the heterogeneous composition of human ASCs to determine specific subpopulation(s) with an enhanced capability to osteogenic differentiation. Such specific subpopulation(s) could be used to ameliorate healing in critical size bone defects as standard procedures are not sufficient for a positive outcome. For this purpose, the following

approaches were pursued:

- Analysis of osteogenic differentiation of 20 human ASC lines using the innovative technique of mass cytometry operating with an already established antibody panel including MSC and osteogenic markers and already optimized established protocols.
- Perform developmental paths in order to monitor expression of different protein markers during osteogenic differentiation in the 20 human ASC lines.
- Determination of a combination of markers characteristic for the subpopulation of ASCs with enhanced osteogenic potential.
- *In vitro* adipogenic differentiation of several ASC lines and analysis with real-time quantitative PCR of MSC and adipogenic markers.
- *In vitro* chondrogenic differentiation of several ASC lines.

1.5 Previous work

This Doctoral Thesis uses the data obtained in the author's Master Thesis [40]. That work performed an osteogenic differentiation experiment with adipose-derived stem cells using the CyTOF technique. This Doctoral Thesis performs a more thorough analysis of the data set using new state-of-the-art algorithms. This gives further evidence to the assumption that specific subpopulations more prone to osteogenic differentiation within the heterogeneous population of ASCs exist suggested in the author's Master Thesis are valid.

2 Methods

The following methods are identical to the ones used in the Author's Master Thesis [40] and were complemented and adapted for this Doctoral Thesis which is a continuation of that work.

2.1 Generation and culture of human adipose-derived stem cells

Thirty adipose tissue samples were obtained from healthy, not diabetic human donors undergoing lipoaspirations and lipectomies [41, 25]. Twenty-six patients were female and four were male. From those fat tissues adipose-derived stem cell lines (ASCs) were established in the laboratory. 21 cell lines were used for this Doctoral thesis. Part of them have been previously characterized [41, 25] whereas others were characterized for this project. Human ASCs were cultured in Dulbecco's Modified Eagle Medium (DMEM, supplemented with 10% of Fetal Calf Serum (FCS), 1% of antibiotics: 100x Penicillin, 100x Streptomycin, and 1% L-glutamine 200nM: ASC Medium), which was changed every 2-3 days. Cells were passaged when they reached about 80% confluence with 1x Trypsin for 5min at 37°C. Cells were incubated in an atmosphere with 95% humidity and 5% CO2 at 37°C. ASCs were frozen in ASC Medium supplemented with 1% dimethyl sulfoxide (DMSO). All experiments were performed with ASCs below passage 10.

2.2 Reverse transcription and real-time quantitative PCR

RNA was isolated using RNeasy mini Kit (Qiagen) following the manufacturer's instructions. After isolation, reverse transcription was carried out with a GeneAMP PCR System (2hours 50°C, 10min 72°C) using 0.5g RNA, 0.5 g/ul oligo-dT primers, dNTP mix (10 mM), DTT (0.1M), 5xFS Buffer, RNA inhibitor (20 U/ul) and SuperScript III (200 U/ul). Real-time quantitative PCR (RTQ-PCR) was performed using SYBR Green and specific primers (Tab. 2) with a Rotor Gene PCR machine. Cycling conditions were: 95°C for 5s, 60°C for 30s, and 72°C for 30s, for a total of 40 cycles. Analysis of the melting curves excluded unspecific amplification and primer dimer formation. Gene expression was normalized to GAPDH expression and calculated using the $2^{-\Delta\Delta ct}$ and $2^{-\Delta ct}/10^{-3}$ methods [42].

2.3 Osteogenic differentiation

In order to assess osteogenic differentiation, 21 ASC lines were cultured with StemPro® Osteogenesis Differentiation Kit (Gibco) for a period of 21 days. The medium was changed every 3-4 days. Cells were cultured in 6-well plates and collected for gene expression analysis at the following time points: day 0 (d0), d1, d2, d3, d4 (200000 cells/well), and d7, d14, d17, d21 (100000 cells/well). In order to collect an equal amount of cells at these time points, late time points were seeded with less cells as they were cultured longer. RNA was extracted as described before and gene expression was monitored by RTQ-PCR (Sec. 2.2). For the detection of calcium deposition, cells were cultured in 24-well plates (10000 cells/well). Cells to be stained with Alizarin red and

Table 2: Human primer list.

Gene	Forward primer	Reverse primer
GAPDH	5'-ACCACAGTCCATGCCATCAC-3'	5'-TCCACCACCCTGTTGCTGTA-3'
CD105	5'-CAGCAGTGTCTTCCTGCATC-3'	5'-AGTTCCACCTTCACCGTCAC-3'
CD73	5'-CTCCTCTCAATCATGCCGCT-3'	5'-CCCAGGTAATTGTGCCATTGT-3'
CD44	5'-GATCCACCCCAATTCCATCTGTGC-3'	5'-AACCGCGAGAATCAAAGCCAAGGCC-3'
CD106	5'-GGACCACATCTACGCTGACA-3'	5'-TTGCATGTGATCGGCTTCCC-3'
CD146	5'-CAACAGCACCTCCACAGAGA-3'	5'-GTGATCTCCTGCTTCCCTGA-3'
CD90	5'-TGAATACAGACTGCACCTCCC5-3'	5'-CTTGACGGGTGAGGCTAGGA5-3
EGFR	5'-GGTGAGCCAAGGGAGTTTGT-3'	5'-TCTTAGGCCCATTCGTTGGAC-3'
PDGFRα	5'-CGGAGGAGAAGTTTCCCAGAG-3'	5'-CTGCTCACTTCCAAGACCGT-3'
Osteocalcin	5'-CACTCCTCGCCCTATTGGC-3'	5'-CCCTCCTGCTTGGACACAAAG-3'
AP	5'-CTGGTAGTTGTTGTGAGCAT-3'	5'-CCCAAAGGCTTCTTCTTG-3'
RUNX2	5'-GAACCCAGAAGGCACAGACA-3'	5'-GGCTCAGGTAGGAGGGCT-3'
PPARy	5'-CCT GCT ACA AGC CCT GGA-3'	5'-CTG CAC GTG TTC CGT GAC-3'
FAB4	5'-GTG GGC TTT GCC ACC A-3'	5'CCT GGC CCA GTA TGA A-3'
APM1	5'TGT TGC TGG GAG CTG TTC TAC TG-3'	5'-ATG TCT CCC TTA GGA CCA ATA AG-3'

control cells (cultured with ASC medium) were both cultured in triplicates for the time points 14, 17, and 21 days.

2.3.1 Detection of calcium deposition by Alizarin Red staining

As mentioned before, calcium deposition was assessed after 14, 17, and 21 days of differentiation. First of all, cells were washed with PBS, fixed with 4% formalin (Roth) for 30min at room temperature (RT) and then incubated with Alizarin Red solution (pH 4.16, 40mM; Sigma) for 20min at RT. Afterwards cells were washed with distilled water (ddH_2O) and let dry. Pictures were taken with an Epson expression 1640 XL scanner.

2.4 Adipogenic differentiation

Adipogenic differentiation was induced with StemPro® Adipogenesis Differentiation Kit (Gibco). As for the osteogenic differentiation 21 human ASCs were cultured either into 6-well plates (for RNA analysis) or in triplicates into 24-well plates for detection of lipids by Oil Red O staining. The medium was changed every 3-4 days. The same amount of cells was distributed as described for osteogenic differentiation. RNA samples were taken at d0, d1, d2, d3, d4, d7, d14, d17, d21 whereas at day 14, 17, and 21 lipids were stained with Oil Red O.

2.4.1 Detection of lipids by Oil Red O staining

For the detection of lipids cells were washed with PBS and then fixed with 10% formalin (Roth) for 5min. The formalin was removed and added fresh to the cells for another 60min at RT. After fixation, cells were washed twice with ddH_2O and then rinsed twice with 60% isopropanol. Cells were thereafter let dry completely and then incubated for 10min with Oil Red O working solution

(6ml Oil Red O stock solution plus 4ml ddH_2O). Next cells were washed four times with ddH_2O. For quantification of adipogenic differentiation pictures were taken (in 500ul ddH_2O) using Leica microscope DMIL LED with Leica camera DFC 425 C. For each well 12 pictures were taken at a magnitude of 20X, Oil Red stained cells were counted and the mean of the triplicates was reported.

2.5 Chondrogenic differentiation

Chondrogenic differentiation was induced by StemPro® Chondrogenesis Differentiation Kit (Gibco). In contrast to the osteogenic and the adipogenic differentiation, the 21 cell lines were given into TPP Tubespin Bioreaktors with filters (200000 cells/tube) in order to assess cartilage formation. Cells were centrifuged at 500x g for 10min at RT and cultured as pellets in chondrogenic inducing medium. For each time point (day 14, d17, and d21) two tubes were prepared: one with chondrogenic medium and the other one with ASC medium serving as a control. The medium was changed every 3-4 days.

2.5.1 Detection of cartilage by Alcian Blue staining

After 14, 17, and 21 days, cells cultured in chondrogenic conditions formed pellet-like clumps at the bottom of the tube. Carefully the pellets were washed with PBS and fixed with 10% formalin (Roth) for 20min at RT. Afterwards the pellets were transferred into 1.5ml tubes, embedded into 2% agarose and incubated on ice for 30min. Afterwards the solid agaroses containing the cell-clumps were transferred into histocassettes, put in 70% ethanol and stored at -20°C. Then histocasettes were washed in PBS and given into a tissue processing apparatus. Thereafter, the agaroses with the cells were embedded into liquid paraffin, left at RT until they were solid and then stored at -20°C. Paraffin wax sections were cut at 5 um and given onto microscope slides. The slides were deparaffinized via incubation in xylol for two times, in 100% ethanol three times, in 96% ethanol one time and once in 70% ethanol. After deparaffinization, cells were rehydrated in PBS. Then, slides were incubated in 1% Alcian Blue solution for 60min at RT. Next slides were rinsed three times with 0.1% HCl, neutralized with ddH_2O, and air dried. Pictures were taken using Leica DM6000B microscope and Leica DFC 425 C camera.

2.6 Analysis of human adipose-derived stem cells with cytometry by time-of-flight

2.6.1 Antibody panel

For the analysis of undifferentiated and osteogenic differentiated human ASC lines by CyTOF an antibody panel was used which was already established in the laboratory prior this Doctoral Thesis (Tab. 3, [43, 40]).

Table 3: Antibody panel.

Antigen target (human)	**Location of the antigen**	**Clone number**	**Company**	**Elemental isotope**	**Final concentration (for 1mio cells in 100$\mu\ell$)**	**Final concentration (for >10mio cells in 300$\mu\ell$)**
CD19	Surface	HIB19	Biolegend	^{142}Nd	1/1600	1/800
CD11b	Surface	ICRF44	Fluidigm	^{144}Nd	1/1600	1/800
CD73	Surface	AD2	Biolegend	^{146}Nd	1/800	1/400
CD146	Surface	P1H12	Fluidigm	^{155}Gd	1/100	1/50
NG2	Surface	7.1	Santa Cruz	^{150}Sm	1/400	1/200
CD45	Surface	HI30	Fluidigm	^{154}Sm	1/3200	1/1600
CD79α	Surface	HM47	Biolegend	^{156}Dy	1/800	1/400
CD106	Surface	STA	Biolegend	^{158}Gd	1/800	1/400
PDGFRα	Surface	D13C6	Fluidigm	^{160}Gd	1/800	1/400
CD90	Surface	5E10	Fluidigm	^{161}Dy	1/800	1/400
STRO-1	Surface	STRO-1	Biolegend	^{163}Dy	1/800	1/400
CD271	Surface	ME20.4	Biolegend	^{165}Ho	1/800	1/400
EGFR	Surface	AY13	Biolegend	^{167}Er	1/800	1/400
CD44	Surface	IM7	Fluidigm	^{171}Yb	1/800	1/400
CD38	Surface	HIT2	Fluidigm	^{172}Yb	1/200	1/100
CD14	Surface	M5E2	Fluidigm	^{175}Lu	1/800	1/400
CD105	Surface	43A3	Biolegend	^{176}Lu	1/800	1/400
RUNX2	Nuclear	S533	GeneTex (GTX81326)	^{153}Eu	1/800	1/400
AP	Cytoplasmic	TRA-2-49/6E	Stem Cells (60066)	^{169}Tm	1/1600	1/800

2.6.2 Osteogenic differentiation experiment with 20 human ASC lines

For the osteogenic differentiation experiment 20 human ASC lines were cultured over a period of 4 days under osteogenic differentiation conditions. For the time points day 0, d1, d2, d3, d4 one 10cm dish containing 1.5 mio cells was prepared for all the 20 ASC lines for a total of 100 dishes in culture. Cells were split into the dishes at d0 and cultured with StemPro® Osteogenesis Differentiation medium, each plate with 8ml medium which was never changed over the period of the experiment (4 days). Day 0 cells (that means untreated cells) were immediately collected and further treated (Fig. 3).

Barcoding As depicted in Fig. 3, each day cells were collected and barcoding was performed using Cell-ID 20-Plex Pd Barcoding Kit (Fluidigm). A barcoding plan was developed prior starting the experiment (Tab. 4). For that, cell lines were divided into good, bad and intermediate groups based on Alizarin red staining from 21 days of osteogenic differentiation as described before. Since the barcoding kit had 20 different codes we ended up having 5 tubes each containing 4 cell lines with 5 time points. Within one tube, each cell line had its own barcode for each time point (Tab. 4).

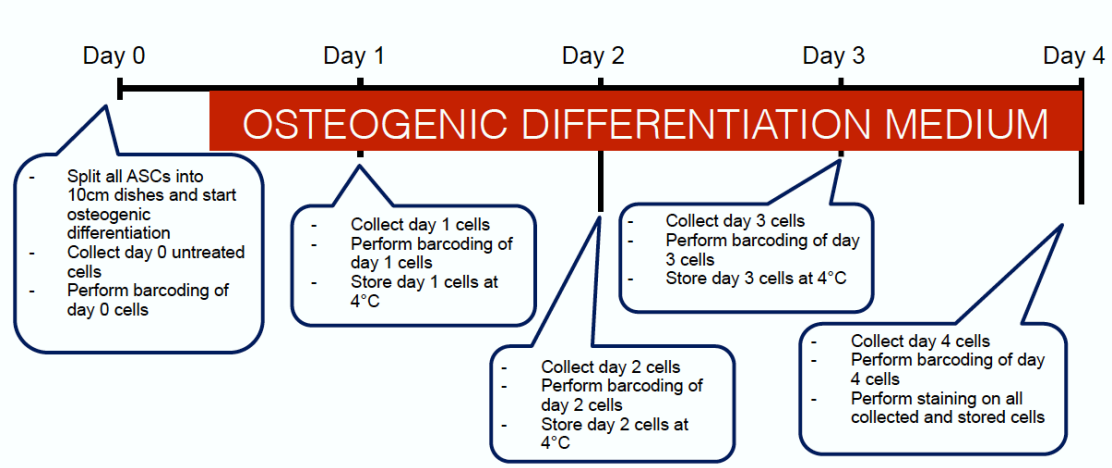

Figure 3: Illustration of the osteogenic differentiation of 20 human ASC lines followed by CyTOF analysis. After cell staining at day 4 cells were stored at 4°C until CyTOF analysis was performed.

Table 4: Barcoding plan.

		barcode				
cell line name	**differentiation potential**	**day 0**	**day 1**	**day 2**	**day 3**	**day 4**
Tube 1 contains cell lines:						
F4	good	1	5	9	13	17
F19	bad	2	6	10	14	18
F8	intermediate	3	7	11	15	19
F9	not determined yet	4	8	12	16	20
Tube 2 contains cell lines:						
F5	good	1	5	9	13	17
F27	bad	2	6	10	14	18
F14	intermediate	3	7	11	15	19
F16	not determined yet	4	8	12	16	20
Tube 3 contains cell lines:						
F15	good	1	5	9	13	17
F10	bad	2	6	10	14	18
F17	intermediate	3	7	11	15	19
F23	not determined yet	4	8	12	16	20
Tube 4 contains cell lines:						
F18	good	1	5	9	13	17
F29	intermediate	2	6	10	14	18
F32	intermediate	3	7	11	15	19
F30	not determined yet	4	8	12	16	20
Tube 5 contains cell lines:						
F22	good	1	5	9	13	17
F28	intermediate	2	6	10	14	18
F31	intermediate	3	7	11	15	19
F11	intermediate	4	8	12	16	20

The barcoding protocol was the following: cells were washed with PBS and incubated with Cell-ID™ Cisplatin for 10min at RT. Afterwards cells were fixed with MaxPar® Fix I Buffer for 10min at RT, washed with MaxPar Barcode Perm Buffer, and incubated with its specific barcode (Tab. 4) for 30min at RT.

Staining protocol At the last day of the experiment, all barcoded cell lines were pooled into the 5 tubes according to the barcoding plan (Fig. 3 and Tab. 4) to be stained all together. Cell staining was performed with the antibody panel (Tab. 3) following the 3 protocols from MaxPar®: Cell Surface Staining Protocol, Cytoplasmic/Secreted Antigen Staining Protocol, and Nuclear Target Staining Protocol (Fluidigm) as established prior in the laboratory [40]. Nevertheless, some adjustments at the protocol were performed since the amount of cells was much higher than what usually stained: Fixation times for each staining protocol were reduced and staining were performed in 300ul end volume instead of 100ul and antibody concentrations were doubled (Tab. 3). In short, cells were incubated with the cell surface antibody cocktail for 30min at RT. Afterwards, cells were washed with MaxPar® Cell Staining Buffer. Next, cytoplasmic antigen staining was performed: cells were fixed with MaxPar® 1X Fix I Buffer for 10min at RT (instead of 30 min). Then, cells were washed in MaxPar® Perm-S-Buffer and incubated with the cytoplasmic antibody (Tab. 3) for 30min at RT. Upon washing with MaxPar® CSB for the nuclear target staining, cells were fixed with eBioscience FoxP3 Fixation/Permeabilization Buffer (1X) for 10min at RT (instead of 45min). Cells were washed with eBioscience Permeabilization Buffer and incubated with the nuclear target antibody (Tab. 3) for 60min at RT. After the staining, cells were washed in MaxPar® CSB and resuspended in MaxPar® Fix and Perm Buffer containing Cell-IDTM Intercalator-IR and stored at 4°C until data acquisition. Data acquisition was made with a CyTOF 2 Mass Cytometer by expert people at the Mass Cytometry Facility of the University of Zurich.

3 Materials

The materials used for the experiments are listed in Table 5.

Table 5: Material list.

Materials	Company	Catalog number
Cell culture		
10cm dishes	Corning	
6-well plates	Costar	3516
24-well plates	Thermo scientific 1	42475
15 ml tubes	TPP	91014
Dulbeccos modified eagle medium-DMEM	Pan Biotech	P04-03550
100x Penicillin	Biowest	L0022-100
100 x Streptomycin	Sigma	
L-glutamine 200nM	Sigma	G7513
Fetal calf serum (FCS)	Pan	
Trypsin 10x	Sigma	T4174
Dimethylsulfoxide-DMSO	Sigma	D4540
PBS	Kantonsapotheke Zürich	
Differentiation medium		
StemPro® Osteogenesis Differentiation Kit	Gibco	A-10072-01
StemPro® Adipogenesis Differentiation Kit	Gibco	A-10070-01
StemPro® Chondrogenesis Differentiation Kit	Gibco	A-10071-01
Staining		
Oil Red O	Sigma	O 0625
Alizarin red	Sigma	A5523
Formalin	Roth	
Alcian Blue	Sigma Aldrich	A5268
RNA Isolation, reverse transcritpion, qPCR		
RNase mini kit	Qiagen	74106
Qiashredder(250)	Qiagen	79656
Oligo-dT Primers	Invitrogen	
dNTP mix	Qiagen	201900
DTT	Qiagen	
5 x FSB	Invitrogen	
RNA Inhibitors	AB	100021540
SuperScript® III	Invitrogen	18080093
Sybr Green	Qiagen	205076
CyTOF		
1.6% formalin	Roth	
Cell-ID 20-Plex Pd Barcoding Kit	Fluidigm	201060
MaxPar® Cell Staining Buffer	Fluidigm	201068
MaxPar® Fix and Perm Buffer	Fluidigm	201067
MaxPar® Water	Fluidigm	201069
Cell-ID™ Intercalator-Ir	Fluidigm	201192A [125M] or 201192B [500 M]
Cell-ID™ Cisplatin	Fluidigm	201064
MaxPar® Fix I Buffer (5X)	Fluidigm	201065
MaxPar® Perm-S Buffer	Fluidigm	201066
eBioscience FoxP3 Fixation/Permeabilization Concentrate and Diluent	eBioscience	00-5521
eBioscience Permeabilization Buffer (10X)	eBioscience	00-8333

4 Results

In general, the capability of bone fracture healing differs substantially among different patients. On the one hand some patients are able to regenerate bone rapidly, on the other hand other patients experience delayed or even non-union. Why are there such differences? In orthopaedic surgery, adipose-derived mesenchymal stem cells (ASCs) are reported to be a highly effective basis for bone regeneration. Investigation of ASCs obtained from several patients show that all of them fulfil the criteria in accordance with the International Society for Cellular Therapy (ISCT) of mesenchymal stem cells [9], but they range strongly in their osteogenic differentiation potential. This leads to the question, why ASCs isolated from different patients with a defined marker expression (from the ISCT) show varying abilities for bone regeneration.

4.1 Characterization of adipose-derived stem cells

In order to have a better understanding why such differences in bone regeneration exist, a characterization of ASCs isolated from 21 patients was performed. First, gene expression levels of selected markers were measured in undifferentiated ASCs using real-time quantitative PCR (Fig. 4). Classical MSC markers such as CD73, CD105, CD90, and CD44 were measured. As depicted in Fig. 4, the expression profiles of the mentioned markers show varying levels in the different ASC lines and therefore confirmed their heterogeneity. The marker CD90 generally showed a low expression profile in all the cell lines whereas CD105 showed a range of low to high expression. For example, the line F09 displayed a low expression in the markers CD73, CD105, and CD90 but had a high expression in CD44. In contrast, F32 had low expression levels for CD73 and CD90, and intermediate expression levels in CD105 and CD44.

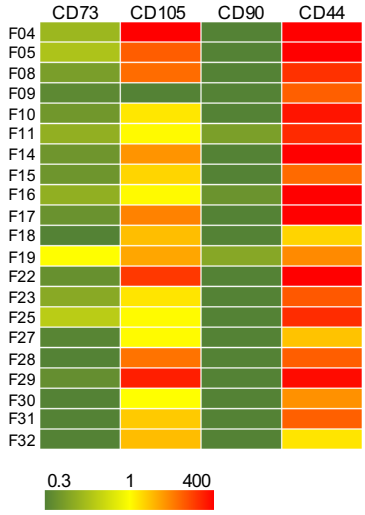

Figure 4: Heatmap for mesenchymal stem cell markers from 21 ASC lines in their undifferentiated state. Expression profiles were evaluated using the $2^{-\Delta ct}/10^{-3}$ method [42].

For further characterization, the multipotency of the 21 ASC lines was investigated. To be precise, each cell line was cultured in particular conditions in order to assess their ability to differentiate into osteoblasts, adipocytes, and chondrocytes.

4.1.1 Osteogenic differentiation

In order to assess the differentiation capacity into osteoblasts, 19 ASC lines were cultured in osteogenic conditions for 14, 17, and 21 days. Calcium deposition was evaluated by Alizarin red staining at the indicated time points (Fig. 5). Five cell lines already showed a calcium deposition at day 14 and 17 (Fig. 5A). Therefore, they were classified as cell lines with a good osteogenic differentiation ability. Six lines were categorized as bad osteogenic differentiation lines, since Alizarin red staining was negative even after 21 days of differentiation (Fig. 5C). The remaining 8 cell lines were positive for Alizarin red staining only after 21 days of differentiation and were therefore categorized as intermediate differentiating lines (Fig. 5B). The classification in good, bad, and intermediate osteogenic differentiating lines is summarized in Tab. 6.

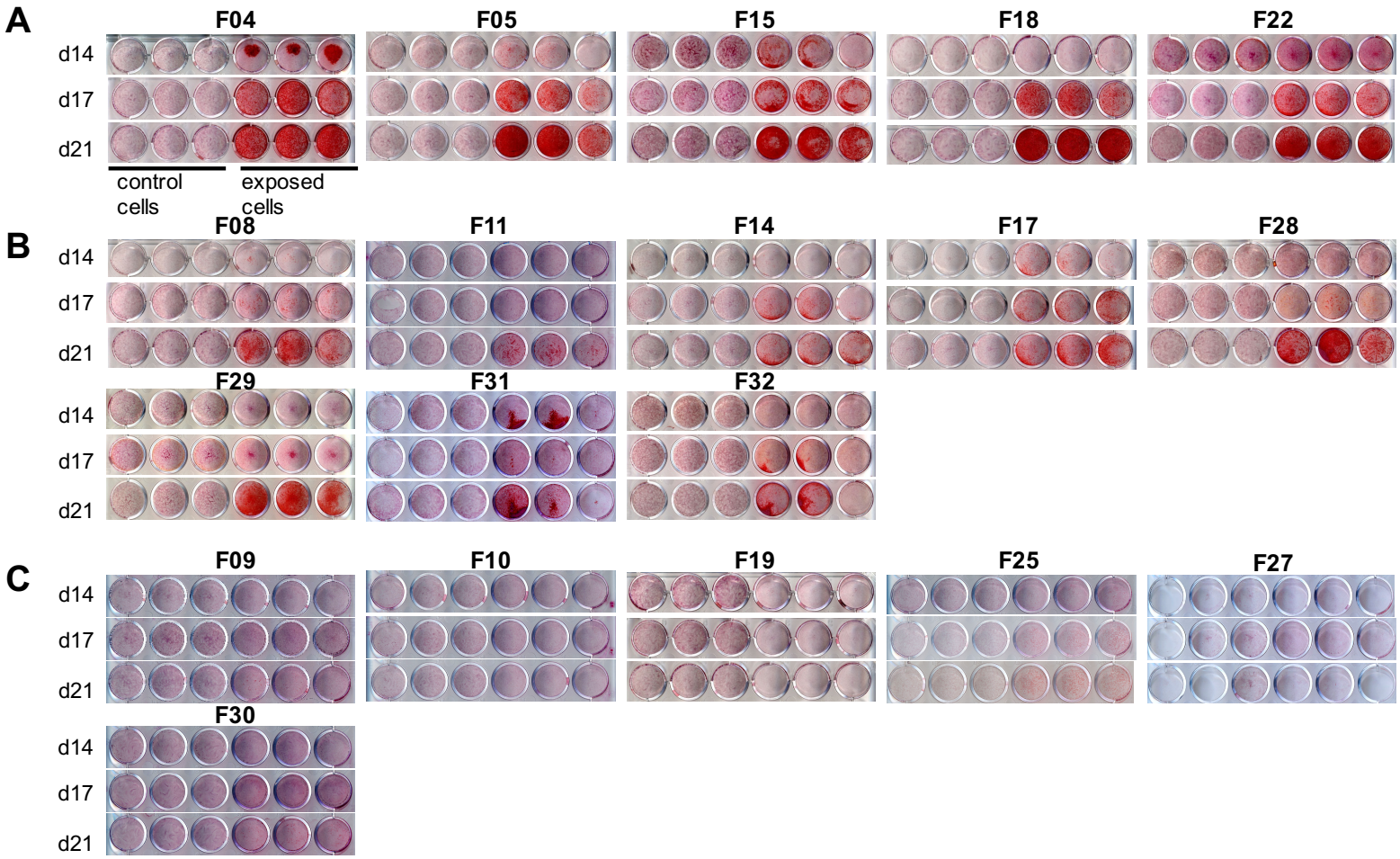

Figure 5: *In vitro* osteogenic differentiation over a period of 21 days for 19 ASC lines. Cells were cultured in triplicates for both: control cells in ASC medium (left) and cells differentiating in osteogenic medium (right). Alizarin red staining was performed after 14, 17, and 21 days. ASCs were classified in good (A), intermediate (B), and bad (C) differentiating lines.

Table 6: 19 ASC lines classified into three groups (good, intermediate, and bad) according to their calcium deposition detected by Alizarin red staining after 21 days of osteogenic differentiation.

good	**intermediate**	**bad**
F04	F28	F19
F05	F29	F27
F15	F32	F10
F18	F14	F09
F22	F08	F30
	F17	F25
	F31	
	F11	

Next, gene expression of selected markers was assessed for 21 ASC lines at different time points during osteogenic differentiation over 21 days (Fig. 6). The stated mesenchymal stem cell markers from the ISCT CD73, CD105 and CD90 as well as MSC marker CD44 were in general down-regulated over the period of 21 days of differentiation. Nevertheless, the expression levels of these markers differed greatly between the ASC lines. For example, the ASC line F04 showed a down-regulation of the markers CD73 and CD105 already at d7, whereas CD90 level was not decreased until d17. CD44 revealed a fluctuating profile in this line. In contrast, the line F27 presented increasing expression levels for all four mesenchymal stem cell markers. As for the ISCT markers, also osteogenic differentiation markers displayed dissimilarities in expression levels (Fig. 6). For example, the line F08 showed increasing expression of osteocalcin and RUNX2 from the first and for AP from the second day of differentiation. In opposition to F08, F11 displayed an upregulation of AP only at d14, whereas the markers osteocalcin and RUNX2 were not up-regulated over the whole time of differentiation. For F17 no trend could be observed, all three osteogenic differentiation markers showed a fluctuating profile.

4.1.2 Adipogenic differentiation

As for the osteogenic differentiation, also adipogenic differentiation was performed for the same 21 ASC lines over a period of 21 days. Fat deposition was assessed at day 14, d17, and d21 by Oil red staining and gene level expression was measured at the same time points like in the osteogenic differentiation (see Sec. 4.1.1).

As in the osteogenic differentiation, also in the adipogenic differentiation heterogeneity could be observed (Fig. 7). For example, F30 showed a slow increase in lipid formation over the 21 days of differentiation, whereas F05 already displayed many lipid aggregations at day 14 (Fig. 7A). Differences could also be seen in the quantification of the adipogenic differentiation (Fig. 7B). F11 and F23 for example showed poor lipid formation, whereas F14 and F16 presented a considerably higher adipogenic differentiation.

Figure 6: Heatmaps for 21 ASC lines for stem cell marker expression (CD73, CD105, CD90, and CD44) and osteogenic differentiation marker expression (Osteocalcin, RUNX2, and AP). Expression levels (low= green, high = red) were measured at day 0, d1, d2, d3, d4, d7, d14, d17, and d21. Depicted is the fold change compared to day 0. Not yet determined marker expression is indicated with a white color.

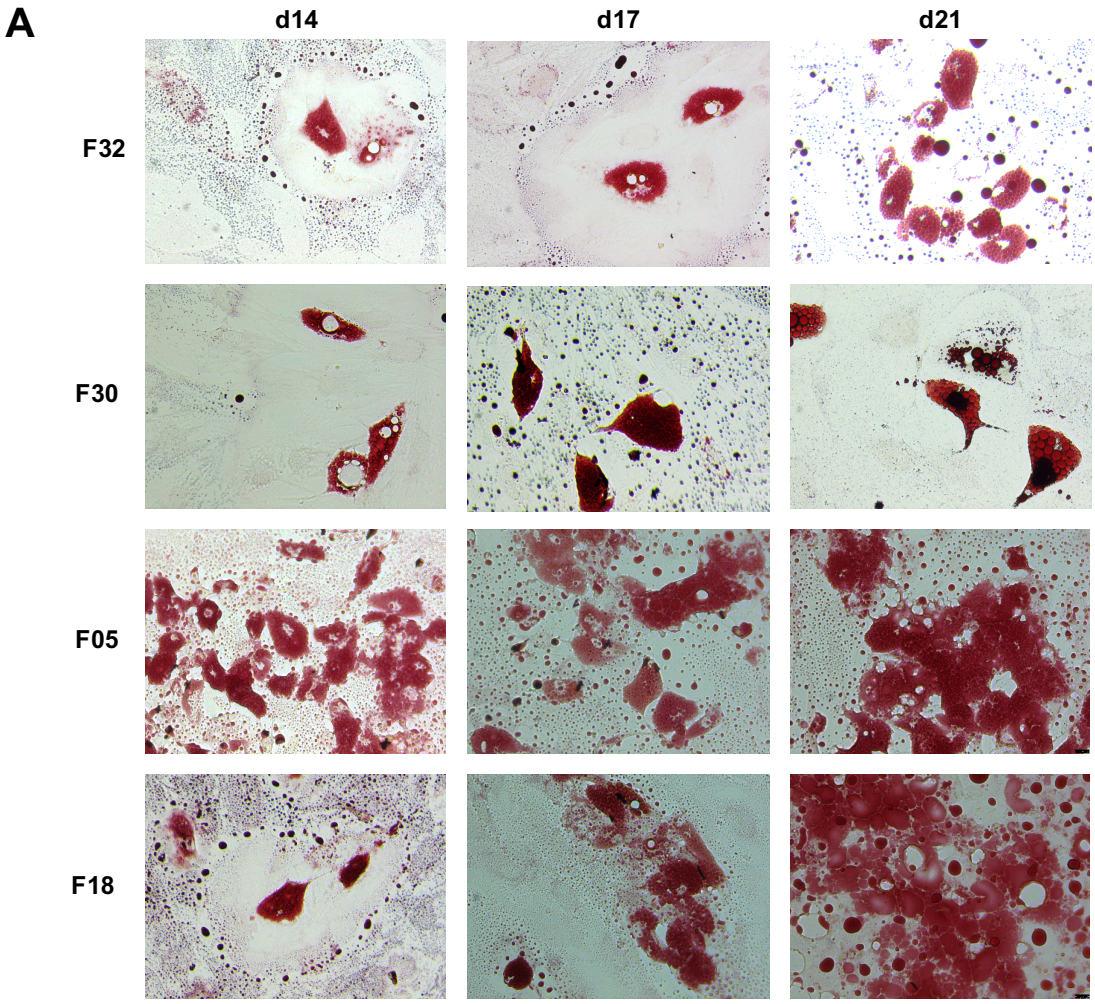

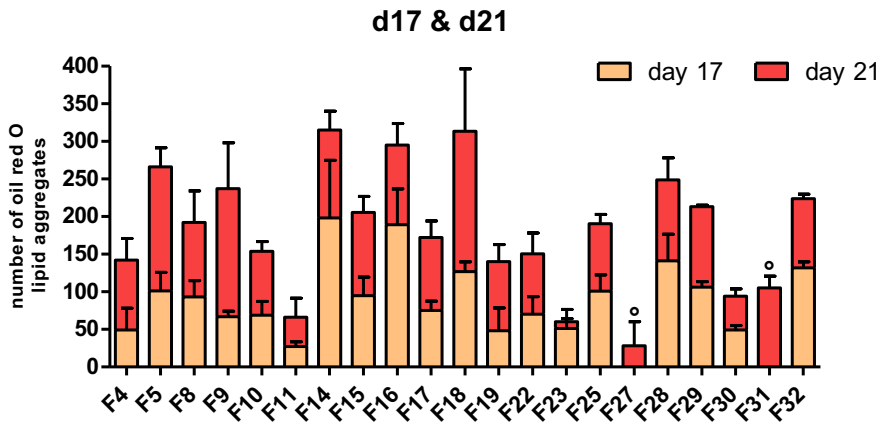

Figure 7: *A* Examples of Oil red O stainings from *in vitro* adipogenic differentiation for the lines F32, F30, F05, and F18 at day 14, d17, and d21. Pictures were taken with a magnification of 20X with Leica microscope DMIL LED with Leica camera DFC 425 C. *B* Quantification of lipid aggregates at 17 and 21 days of adipogenic differentiation from 21 ASC lines. Depicted are the averages of the triplicates, error bars indicate standard deviation of the mean.

Also gene expression levels of different markers during adipogenic differentiation showed differences between the 21 ASC lines (Fig. 8). Expression levels of the stem cell markers CD73, CD105, CD90, and CD44 depicted a general trend of downregulation over the 21 days. For example, F08 showed a downregulation for CD73, CD90, and CD44, but CD105 increased over the period of differentiation. In contrast, in F15 the markers CD73 and CD44 were downregulated, but CD105 increased slightly, and CD90 showed a general high expression level over the 21 days of differentiation. Differences in expression were also observed in the adipogenic differentiation markers. All of them showed a trend of upregulation, although the beginning and the intensity of the upregulation varied (Fig. 8). Expression level of PPARy in F31 for example was increasing already at day 2, expression level for FAB4 and APM1 at day 3. The ASC line F23 on the other hand showed only a slight upregulation of all three markers. F08 displayed a high expression of APM1 towards the end of the differentiation period. PPARy showed only a strong upregulation at day 21 and FAB4 was only slightly increased in this line. Overall, the potential for adipogenic differentiation varied considerably between the 21 investigated cell lines.

Figure 8: Heatmaps for 21 ASC lines for stem cell marker expression (CD73, CD105, CD90, and CD44) and adipogenic differentiation marker expression (PPARy, FAB4, and APM1). Expression levels (low= green, high = red) were measured at day 0, d1, d2, d3, d4, d7, d14, d17, and d21. Depicted is the fold change compared to day 0. Not yet determined markers are indicated with a white colour.

4.1.3 Chondrogenic differentiation

As a last step, also chondrogenic differentiation was performed with 21 ASC lines. Cartilage formation was detected by Alcian blue staining after 14, 17, and 21 days. As depicted in Fig. 9 for three cell lines, only small differences could be seen. For example: Alcian blue staining for F25 was generally stronger than in F23, but considerable differences could not be detected. Therefore, an optimization of the culturing and staining protocols are needed in order to better catch differences between the ASC lines.

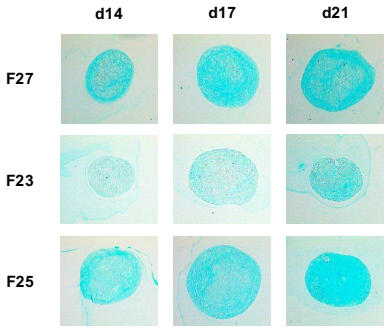

Figure 9: Cartilage formation detection by Alcian blue staining for three ASC lines (F27, F23, F25) during chondrogenic differentiation at day 14, d17, and d21. Pictures were taken with a Leica DM6000B microscope and Leica DFC 425 C camera at a magnitude of 5X.

To sum up, we showed that significant differences exist between the investigated 21 ASC lines not only in their *in vitro* trilineage potential, but also in their marker expression patterns. According to these observations, it can be assumed that the composition of the different ASC lines is highly heterogeneous and that they are probably composed of smaller subpopulations with dissimilar differentiation abilities. As our primary interest was to detect why different patients have different outcomes in bone regeneration, we came to the conclusion that Alizarin red staining and real-time quantitative PCR allow only evaluation of the whole population of the ASCs without taking the existence of subpopulations into account. It is to assume that distinct small subpopulations might have enhanced potential for osteogenic differentiation. These cells would be the ones of interest to be further investigated. For this purpose, the innovative technique of cytometry by time-of-flight (CyTOF), which allows evaluation on a single cell basis, was used to further analyse the selected 20 ASC lines.

4.2 Analysis of adipose-derived mesenchymal stem cells by CyTOF

CyTOF combines classical flow cytometry with mass spectrometry. This novel technology enables therefore real-time analysis of individual cells, which were previously labelled with stable heavy metal isotopes. In theory, mass cytometry has the advantage of having theoretically over 120 detection channels available.

4.2.1 Analysis of undifferentiated adipose-derived mesenchymal stem cells

For the main CyTOF experiment, 20 human ASC lines were exposed to osteogenic medium over a period of four days, collected, and stained with the established antibody panel which included 19 markers (Tab. 3). Data acquisition with mass cytometry provided high dimensional data. The goal of the analysis of this data was to investigate whether the differences between good and bad differentiating ASC lines, based on the outcomes of the Alizarin red staining, were also present on the level of single cells.

The first aim of the CyTOF experiment analysis was to determine whether differences between the two groups of ASC lines, namely the good and the bad, are already present in the undifferentiated state of the cells. In order to analyse the multiparametric CyTOF data, dimensionality reduction algorithm t-SNE was performed for the 20 ASC lines at day 0 (Fig. 10). Figure 10 displays the marker distribution across the t-SNE map for all markers of the antibody panel. Cells strongly expressing the stem cell markers CD73, CD90 and CD105 were located in the upper left side of the cloud. Interestingly, the tyrosine kinase receptors PDGFRa, EGFR, as well as NG2 displayed a similar pattern. Similarly, RUNX2 expressing cells were also located in the upper left corner. The MSC negative markers CD45, CD14, and CD11b depicted no marker expression. Surprisingly, CD19a MSC negative marker displayed a small percentage of cells with high expression (Fig. 10).

In order to approach the question whether there are subpopulations more prone to differentiate into osteoblasts, an algorithm which allows detecting rare cell subsets was needed. A recent approach called CellCnn, which is based on representation learning, offered a substantial methodology to address this question [39]. CellCnn detects rare cell subsets associated with a prior known phenotype (for example healthy or diseased condition) by means of a representation learning approach using high dimensional measurements on a single cell basis as an input. In order to achieve an association between the input of single cell measurements and the known phenotype the algorithm makes use of a convolutional neural network. This network learns to represent a subpopulation through molecular profiles (filters) of single cells in terms of their frequency or presence. The single cells are associated with the phenotype [39].

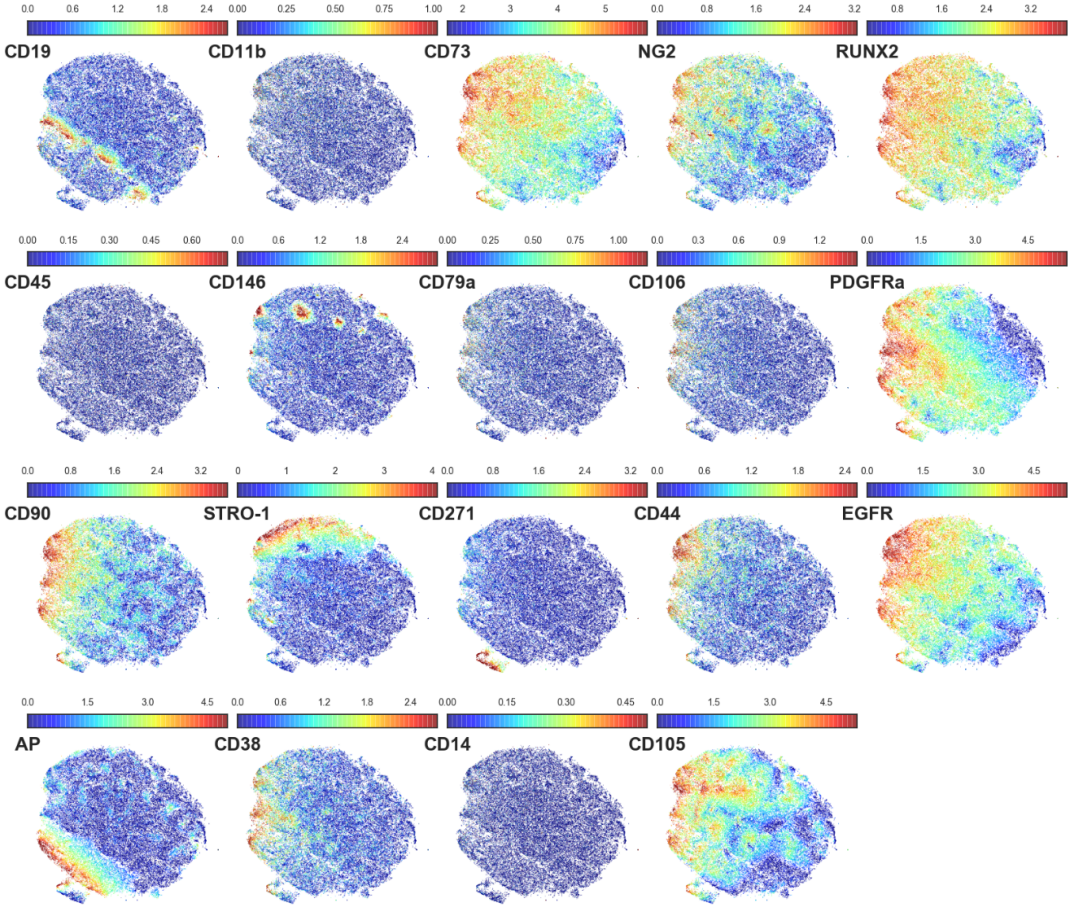

Figure 10: Distribution of the 19 markers across the t-SNE map for 20 ASC lines. Each point represents one cell and they are colour-coded based on their abundance of the indicated marker (red is highly expressed and blue stands for no expression).

In our experimental setting, the classification in "good" and "bad" differentiating ASC lines according to the results of Alizarin red staining (Fig. 5) was used as the phenotype. For the analysis, data from the good and the bad cell lines at day 0 were extracted. Then, CellCnn was trained to be able to identify cell subpopulations that differ in the abundance between the good and the bad group. Five cross-validation repetitions were carried out and three out of them gave a consistent result: Two cell subpopulations were detected that differed significantly between the two groups. Figure 11 depicts the subpopulation which is more abundant in the badly differentiating cell lines on the t-SNE map (subpopulation 1). As it is clear to observe, the MSC markers CD73, CD90, and CD105 are highly expressed by the cells in the upper left corner of the t-SNE cloud. PDGFRa and EGFR are also highly positive in subpopulation 1 within the same area of the cloud (Fig. 11). Interestingly, RUNX2 was also expressed in a similar way. A small percentage of cells strongly expressed the markers CD44, STRO-1, CD146, and NG2, whereas CD11b was less intense. The rest of the markers were not expressed in subpopulation 1 (Fig. 11).

CellCnn detected a second subpopulation, which was more abundant in good differentiating ASC lines (subpopulation 2, Fig. 12). In contrast to subpopulation 1, the MSC markers CD73, CD90, and CD105 were expressed from a smaller amount of cells located in the middle left area of the t-SNE cloud (Fig. 12). Another difference is that a large percentage of cells in the lower left corner of the t-SNE cloud was highly positive for alkaline phosphatase (AP). There were also less cells expressing RUNX2 than in subpopulation 1.

Next, the marker abundance from the two selected subpopulations was compared to the background as depicted in Fig. 13. The most obvious difference between the two subpopulations is the lack of AP expression in subpopulation 1, which was highly expressed in the subpopulation 2. Another example is CD73, which was expressed on a higher level in subpopulation 1 compared to subpopulation 2 (Fig. 13).

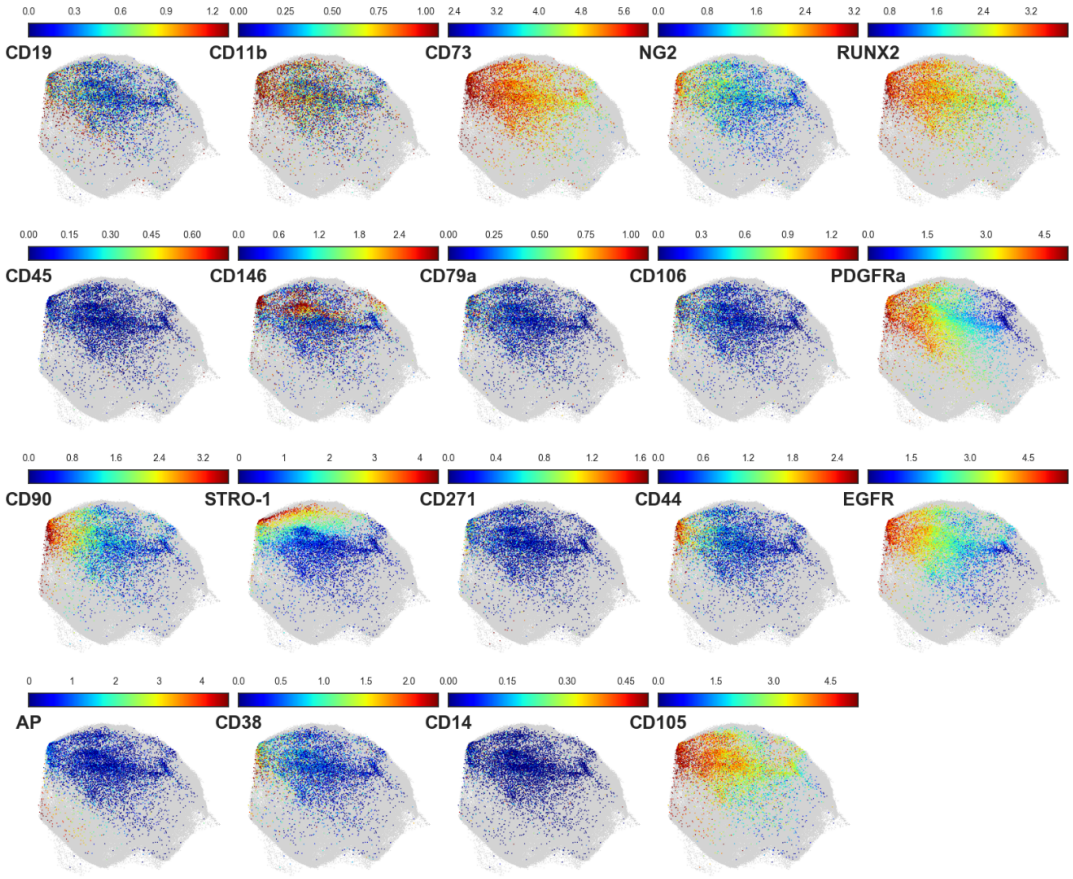

Figure 11: Distribution of the 19 markers across the t-SNE map for the selected subpopulation 1, which was found by CellCnn algorithm to be more abundant in badly differentiating ASC lines. Each point represents one cell and they are colour-coded based on their abundance of the indicated marker (red is highly expressed and blue stands for no expression).

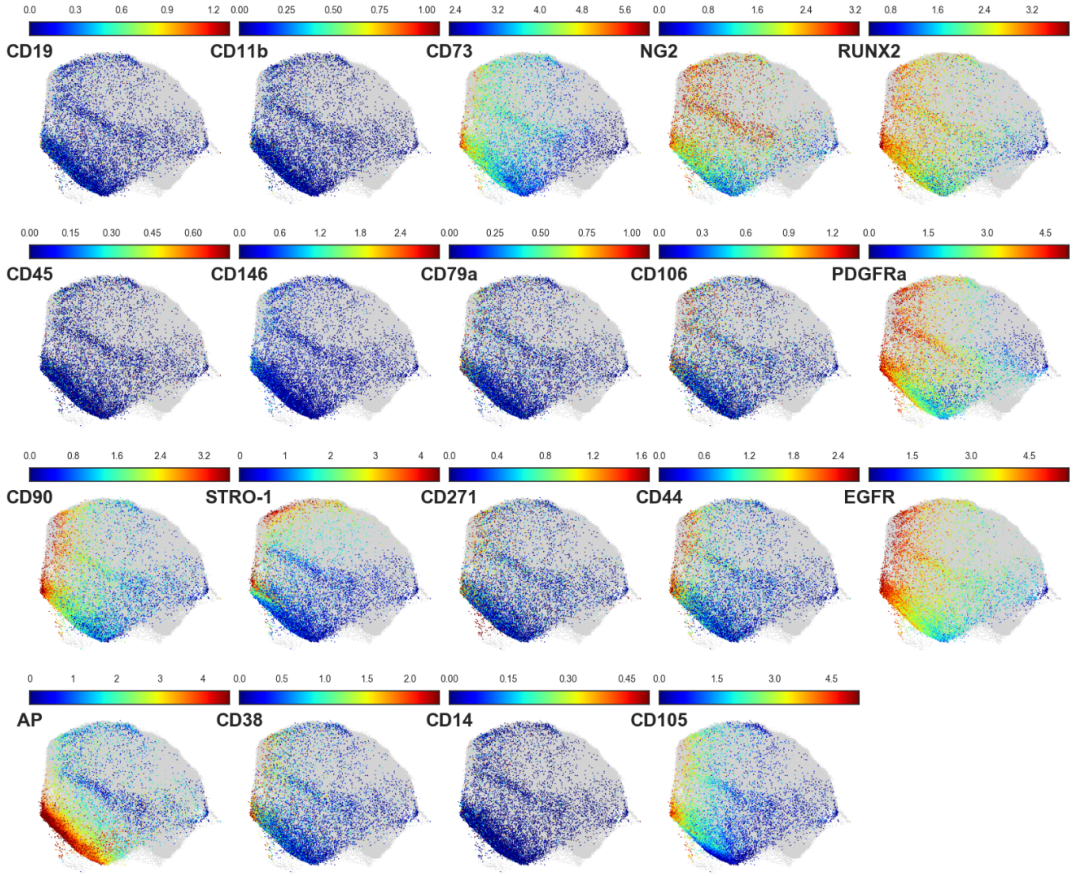

Figure 12: Distribution of the 19 markers across the t-SNE map for the selected subpopulation 2, which was found by CellCnn algorithm to be more abundant in good differentiating ASC lines. Each point represents one cell and they are colour-coded based on their abundance of the indicated marker (red is highly expressed and blue stands for no expression).

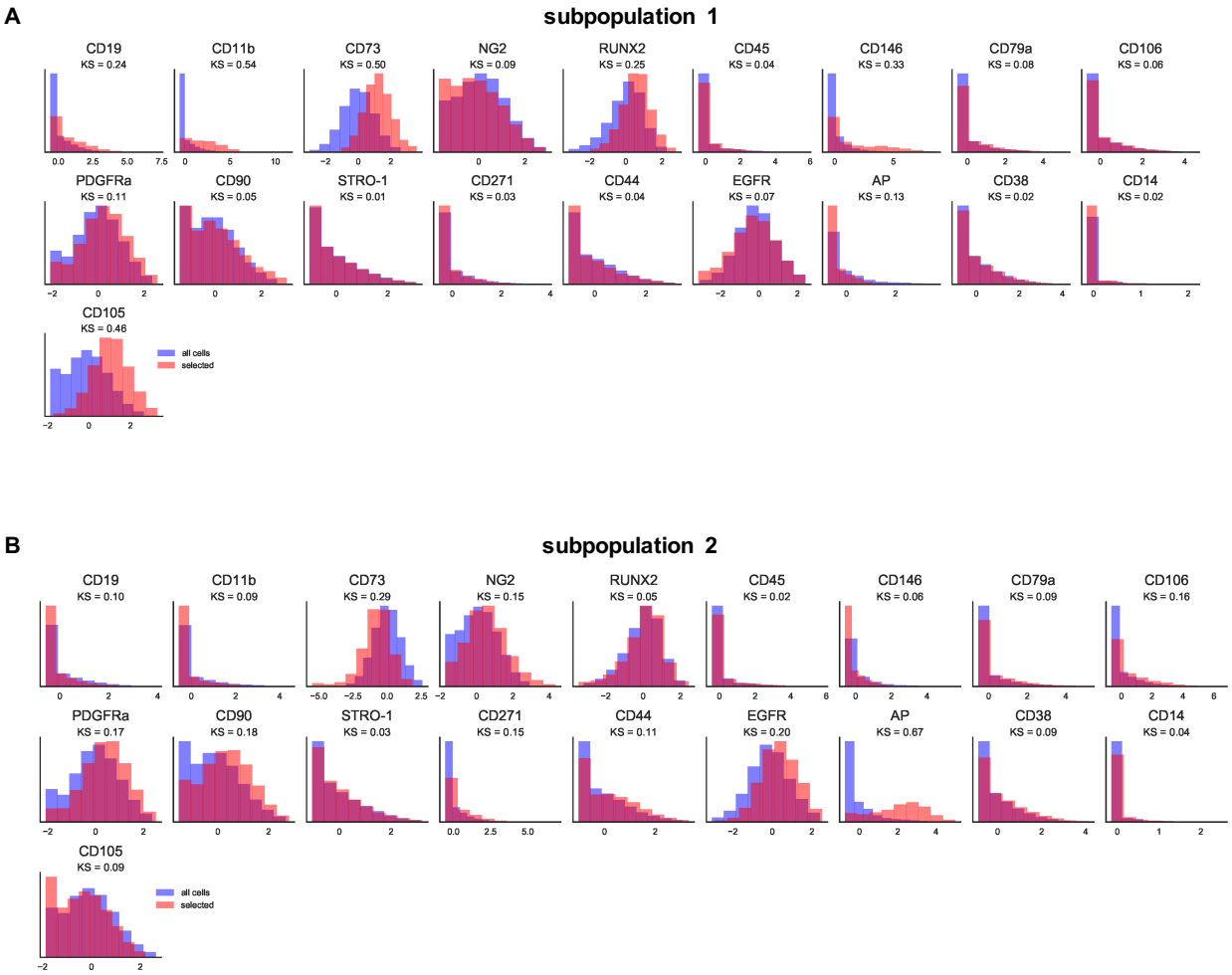

Figure 13: Histograms of marker abundance of 19 markers. Depicted are the intensities of the selected populations (orange) by CellCnn compared to the whole cell subpopulation (background, violet) calculated with the Kolmogorov-Smirnov (KS) two-sample test. *A* Subopulation 1 is more abundant in bad differentiating lines and *B* subpopulation 2 is more abundant in good differentiating lines. The heights are mode normalized.

Another visualization of the two selected subpopulations is displayed in Fig. 14, where the frequencies of the latter are shown within the bad and good ASC lines. The population frequency of subpopulation 1 is noticeably higher in the bad lines compared to the good cell lines. In contrast, subpopulation 2 is clearly more represented in the good ASC lines.

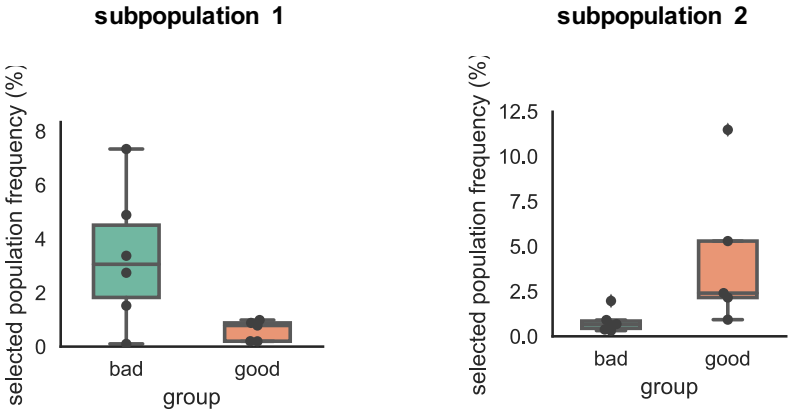

Figure 14: Frequencies (%) of the identified populations 1 and 2 in the bad (green) and the good (orange) groups of differentiating ASC lines at day 0.

In sum, CellCnn identified two subpopulations within the whole population of ASCs, which differed between good and bad ASC lines already in the undifferentiated state of the cells. Hence, it is to assume that there exist probably two (or more not yet determined) subpopulations, whose frequency and marker expression influence the ability for bone regeneration. Presence of subpopulation 1 seems to inhibit osteogenic differentiation by retaining the stem cell markers whereas the cells in subpopulation 2 seem to be prone to differentiate into osteoblasts showing a high level of AP already at day 0. Thus, these observations clearly confirm the hypothesis, that the ASCs obtained from different patients vary in the composition of subpopulations. Therefore, it is to assume, that ASCs are truly highly heterogeneous concerning their composition of subpopulations. In fact, it seems that the different bone healing formation abilities depend on the frequencies of defined small subpopulations.

4.2.2 Analysis of differentiating adipose-derived mesenchymal stem cell

As already reported in Sec. 4.2.1, ASCs showed even in their undifferentiated state dissimilarities in the frequencies of different subpopulations between good and bad osteogenic differentiating ASC lines. In order to further investigate these differences, the two by CellCnn identified subpopulations which displayed different marker expression and frequencies between the two groups of the cell lines were analysed over a period of four days of osteogenic differentiation. In this analysis setup, also the intermediate group was included. As displayed in Fig. 15A, the abundances of the selected subpopulation 1 showed a different pattern in the population percentage

in the course of the four days of differentiation. In fact, the abundance in the bad lines generally increased whereas the good lines displayed only a small upregulation. The intermediate lines seemed to follow the trend of the good lines, as they had a similar abundance only on a slightly higher percentage.

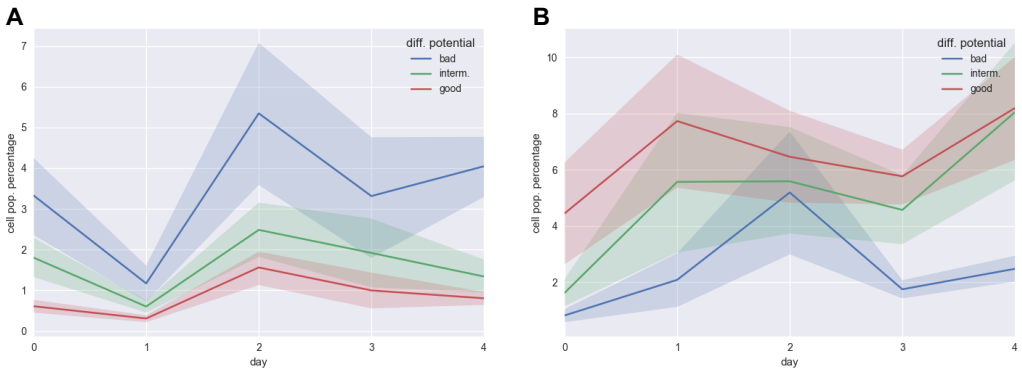

Figure 15: Abundance of selected cell subpopulation 1 (A) and subpopulation 2 (B) in the bad (blue), intermediate (green), and good (red) ASC lines during osteogenic differentiation over four days.

The selected subpopulation 2 also showed a different behavior over the four days of osteogenic differentiation between the different groups of cell lines (Fig. 15B). On the one hand, the good and the intermediate cell lines showed a trend of upregulation in their abundances, on the other hand, the bad lines had indeed an increased in the first two days, reaching almost the level of the intermediate lines, but afterwards they decreased again.

Also of interest, it is to understand how behave the markers within the good, the intermediate, and the bad, during the four days of differentiation. AP for example showed a constant increase over the four days in the good lines (Fig. 16A). In contrast, the bad lines show only a small increase in their AP abundance (Fig. 16A). CD73 showed a general trend of downregulation over the period of four days of osteogenic differentiation, although to a larger extent in the good and intermediate lines (Fig. 16B). In general, the abundance of CD73 is higher in the bad than in the other two cell categories. In comparison to CD73, CD105 did not show obvious differences in their abundances between the different classified cell lines during osteogenic differentiation (Fig. 16C).

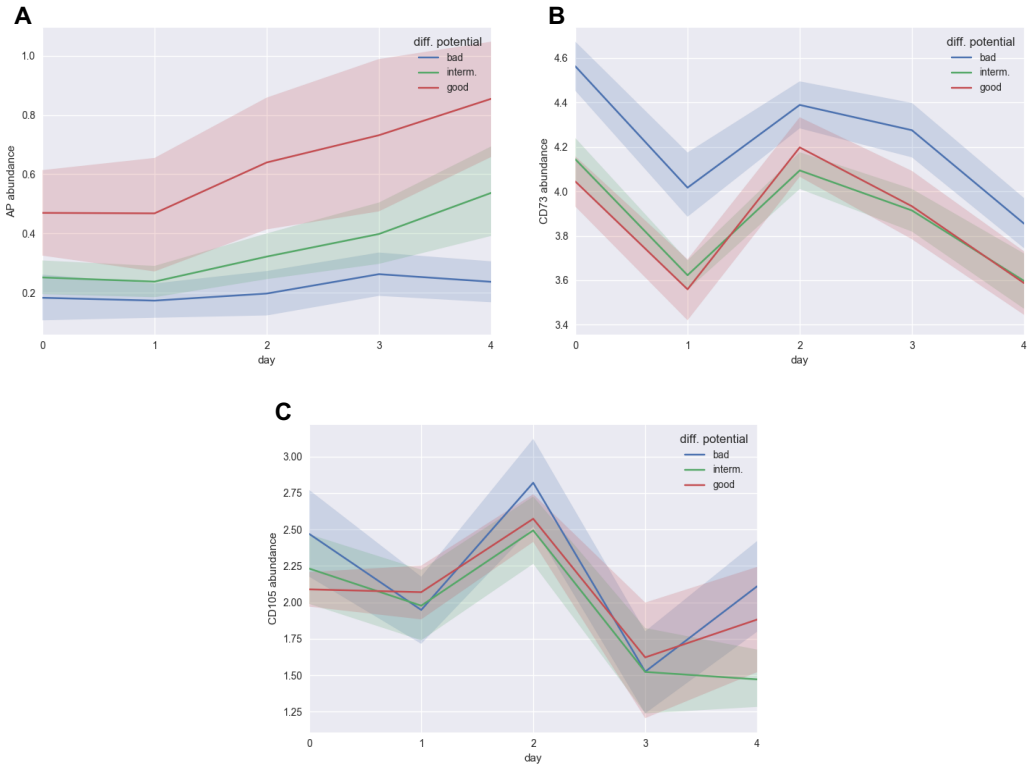

Figure 16: Median expression value of AP (A), CD73 (B), and CD105 (C) during osteogenic differentiation over a period of four days. Depicted are the abundances for the bad (blue), the intermediate (green), and the good (red) classified ASC lines.

To sum up, the results of the mass cytometry analysis displayed that there are indeed differences between good and bad osteogenic differentiating cell lines. This is highlighted not only in the four days of differentiation, but also in the undifferentiated state of the ASCs. CellCnn identified two subpopulations, which need to be deeper investigated in order to be able to clearly explain why there are such big differences between fracture healing outcomes of different patients.

5 Discussion

5.1 Analysis of the heterogeneity of hASCs with multiparametric mass cytometry data

Severe skeletal deficits are associated with a high rate of delayed or non-unions and represent a tremendous clinical challenge [4, 5]. Particularly critical size bone defects, where bridging of the fracture's site remains incomplete without intervention, are still a demanding issue in orthopaedics and reconstructive surgery [6]. Failure of bone regeneration can appear due to substantial bone defects and pathological fractures, but can also be negatively influenced by infection, systemic diseases, and inadequate blood supply [4]. Current therapeutic approaches to achieve skeletal reconstruction involve autogenous, allogeneic, as well as prosthetic constituents. At present, autogenous bone grafts, commonly collected from the crest of the ilium, combined with alloplastic materials are regarded as the gold standard technique for non-healing bone injuries [4, 5]. However, this method brings around drawbacks such as donor site pain, morbidity, and limited supply of bone graft [5]. A recent approach presented cell-based tissue engineering with MSCs, which forged ahead its way in orthopaedic surgery. This technique has been investigated in both large and small animal models [6, 7]. In particular, adipose tissue is stated to be an excellent source of MSCs. The advantages of ASCs are: The easy access for acquisition, the satisfactory quantities of isolated cells, and the straightforward management in cell culture [20].

MSCs are stated to be heterogeneous not only regarding their protein expression, but also due to their morphology and differentiation abilities (reviewed in [24, 23]). These reviews report for instance, that the defined MSC markers from the International Society for Cellular Therapy (ISCT) were indeed present in every isolated cell, but interestingly at varying levels. Clearly, these biomarkers define no inimitably feature for MSCs, but might rather mirror their heterogeneity. Furthermore, differentiation capabilities into specific cell types was reported to be different in the isolated cells [44]. As clinical outcomes in fracture healing are known to differ strongly among individuals, this observation could be an underlying reason. Besides, isolation and culture protocols established for MSCs could also have an impact on the heterogeneous state of the cells. Up to now, research groups used a large variety of protocols for MSCs. Therefore, it is of contradictive nature to directly compare the characterization of MSCs coming from different studies. The protocols could have an influence, for instance, on marker expression among slightly different culture conditions. Moreover, studies have shown that with the established protocols, isolated MSCs not only consist of stem cells, but also of a variety of progenitor cells [45, 44]. Thus, viewing the whole population of isolated cells as stem cells is unsuitable. Because of the heterogeneous composition of MSCs, it is to assume, that MSCs may consist of smaller subpopulations. If the occurrence of a subpopulation is very low in the isolated cells, it could diminish or even vanish under suboptimal culture conditions. For all these reasons protocols need to be ameliorated and standardized. In summary, current protocols and definitions for MSCs do not entirely fulfil the requirements for a reliable use of MSCs in a clinical setting. In order to

approach this issues, it is compulsory to dissect the composition of MSCs on a single cell level in order to get a better characterization of their heterogeneity. Previous studies carried out in our research group have presented for instance that ASCs isolated with adapted protocols such as stromal vascular fraction cells, which have no plastic adherence but ASC marker expression, were likewise able to differentiate towards osteoblasts and endothelial cells and were capable of colonizing a three-dimensional electro spun nanocomposite of poly-lactic-co-glycolic acid [25]. The same study has shown that ASCs from different patients showed dissimilar competences in their lineage propensity, although they were all capable of differentiating into endothelial cells and osteoblasts [25]. Furthermore, another study has presented that defined subpopulations of stem and progenitor cells (NG2+, CD146+, CD45-) can be enriched and then directly applied as a medical treatment without needing *in vitro* expansion [46]. Results from this study confirmed the capacity of amplified NG2+, CD146+, CD45- cells not only to differentiate efficiently towards osteoblasts *in vitro*, but also to migrate into cancellous bone scaffolds and thereby positively influence healing of large bone defects *in vivo* [46]. This study gave evidence that enriched cell subpopulations with stem/progenitor character could be used directly for medical applications. Moreover, the existence of cell subpopulations within ASCs and SVF with enhanced osteogenic differentiation potential was confirmed. This data implies that the variety of differential potentials in ASCs from different donors arises from the heterogeneous populations of ASCs rather than a disturbance of their differentiation ability. Our present hypothesis is that just a few distinct subpopulations have an enhanced bone regeneration capacity. Thereby patients having low quantity of these defined subpopulations may show impaired bone fracture healing for this reason. Therefore, we decided to investigate this hypothesis by analysing 21 ASCs cell lines obtained from different patients.

As anticipated, all of the 21 cell lines expressed the classical MSC markers in their undifferentiated state, nevertheless at varying levels (Fig. 4). Similarly, upon induction of osteogenic differentiation, the analysed cell lines showed very dissimilar potentials to differentiate into osteoblasts, while they were isolated, expanded, and differentiated in exactly the same way (Fig. 5). Gene expression profiles from osteogenic differentiated ASCs reflected a similar pattern (Fig. 6). To sum up, analysing a higher quantity of cell lines again confirmed our hypothesis that a strong heterogeneity between the cell lines exists and that subpopulations with enhanced osteogenic potential are truly present.

Adipogenic differentiation showed that the ASC lines were indeed able to differentiate towards adipocytes, but also in this lineage, their capacity varied widely between the cell lines (Fig. 7). This heterogeneous nature was mirrored not only in the lipid staining but also in the gene expression profiles from the differentiating lines (Fig. 8). Some lines showed good differentiation abilities in both osteoblasts and adipocytes. Others showed good osteogenic, but bad adipogenic differentiation. With this data, no correlation could be established, as there was no obvious trend visible comparing the 21 cell lines. This data clearly indicates that ASCs obtained from individual patients possess different potentials and therefore belongs to the individual nature.

As for the chondrogenic differentiation, all ASC line were able to differentiate towards chondroblasts, but obvious differences such as observed in the osteogenic and adipogenic differentiation could not be detected (Fig. 9). In order to achieve a better characterization of this lineage, the current protocol need further improvement. Therefore, further investigation is needed to evidently see whether there are any differences concerning this lineage or not.

Overall, our data confirmed the trilineage potential of our ASCs. In this Doctoral Thesis, observation of a correlation between the three lineages in one individual patient could not be determined clearly. Some patients had an enhanced potential for bone formation, but their adipogenic differentiation ability was low. On the contrary, some patients showed great differentiation potential in both: Osteogenic and adipogenic differentiation. Comparing all the data from the differentiations, no obvious correlation could be established.

The described data clearly confirmed that the composition of ASCs is truly heterogeneous. Furthermore, it is to assume that not only subpopulations within ASCs with a higher ability for bone formation exist, but also subpopulations with higher propensity towards adipocytes and chondrocytes differentiation may be present. This would also explain why the ASC lines behave so differently, as they probably consist of various subpopulations with dissimilar differentiation abilities.

In order to explore why substantial differences in fracture healing courses are present among different patients, further investigation is urgently needed. In this case, the identification, isolation, and further characterization of subpopulations with enhanced osteogenic potential is of great interest. Subsequently, protocols need to be established which allow an enrichment of these specific subpopulations avoiding the necessity of prolonged *in vitro* cell cultivation. The final objective would be to be able to extract the cells of interest and then directly transplant the enriched subpopulations with enhanced osteogenic potential into critical size bone defects. In order to approach this goal, it is compulsory to study the composition of ASCs on single cell level.

Up to now, dissecting heterogeneous cell populations has been carried out with the widely known method of fluorescence activated cell sorting (FACS). However, FACS has limitations such as only having the capacity to detect a very small number of protein markers. In contrast, the novel technology cytometry by time-of-flight (CyTOF) enables real-time analysis of single cells and has theoretically over 120 detection channels using heavy metal isotopes for marker distinction [47, 29]. This technology allows for the first time a broad characterization of highly heterogeneous populations of cells as it enables functional and phenotypical cell profiling on a single cell resolution. CyTOF has already been successfully used for hematopoietic stem cell characterization ([47, 48]) but was never operated in order to characterize human ASCs. For the very first time, in this Doctoral Thesis, we aimed at illuminating the multi-dimensional marker distribution over the heterogeneous composition of ASCs at single cell level. Furthermore, our goal was to dissect the heterogeneity of human ASCs in order to identify subpopulations of ASCs responsible for osteogenic differentiation. In future, these cells could be applied to ameliorate

treatment procedures of critical size bone defects and as a consequence their clinical outcomes. A tissue engineered approach with ASC subpopulations of enhanced osteogenic potential may be more efficient and less invasive as the currently used standard methods.

For data acquisition with CyTOF, we used a previously established antibody panel including not only classical MSC markers, but also other markers described in relation with MSCs/ASCs (Tab. 3). Not only positive markers, but also defined negative markers were integrated in the panel. Additionally, markers for osteogenic differentiation were included in order to monitor the osteogenic differentiation progression over the four days of the experiment. With this setting, we could for instance confirm that our ASC lines were truly *bona fide* MSCs fulfilling the criteria from the ISCT.

In the primary part of the mass cytometry data analysis we made use of the first developed computational tool for this kind of data, the t-SNE algorithm. This algorithm visualizes multiparametric data of single cells on a low dimensional map. The t-SNE cloud places related cells closer to each other than unrelated ones. Overall, this algorithm allows visualization of CyTOF data by dimensionality reduction in a two dimensional space by conserving the multidimensionality at single-cell resolution. Our data displayed that in the undifferentiated cells the classical MSC markers CD73, CD105, and CD90 were located in a specific region (in the upper left side) within the t-SNE cloud (Fig. 10). Interestingly, the tyrosine kinase receptors PDGFRa, EGFR and also the pericyte marker NG2 seemed to be related to those cells being expressed from cells in the same region of the cloud. Also osteogenic differentiation marker RUNX2 displayed a similar expression.

In order to characterize the ASC lines more accurately, an approach which enables identification of rare cell subsets was needed. We therefore made use of a recently developed algorithm called CellCnn [39]. The latter is able to detect rare cell subsets associated with a prior known phenotype through representation learning by using a convolutional neural network [39]. We first applied this algorithm to our data of the undifferentiated cells of all cell lines using the outcome of the Alizarin red staining as the phenotype. In the analysis of our 20 ASC lines, the endpoint was a good or bad ability for osteogenic differentiation. CellCnn was trained to identify cell subpopulations that differ in abundance between the good and the bad group. Two subpopulations were identified, one that was more abundant in the good, and one that was more abundant in the bad lines.

The identified subpopulation 1, which was found by CellCnn to be more abundant in the bad lines, showed cells intensely expressing the classical MSC markers (Fig 11). In contrast, subpopulation 2, which was more abundant in the good lines, displayed a lower amount of cells expressing these classical markers (Fig. 12). Interestingly, osteogenic differentiation marker AP was highly expressed form a large amount of cells within this subpopulation 2 (Fig. 12). It may be assumed that the cells from the bad lines remained in a kind of stem cell state, as they expressed the MSC markers intensively. In contrast, the good lines seem to be more prone to differentiate into osteoblasts, which was mirrored in their high expression of AP as well as a low

expression of MSC markers.

Summarizing, already in the undifferentiated state of the ASCs, we were able to detect differences between the good and the bad osteogenic differentiating lines. This was illustrated through the two determined subpopulations varying in their frequency and expressing biomarkers differently compared in the good and bad lines (Fig. 11 and 12). These are very promising results, since an immediate identification of the right cells of interest and their enrichment through, for instance, a cell sorting technique could avoid prolonged *in vitro* culturing and could be applied immediately for treatment purposes. Thus, clinical outcomes of critical size bone defects could be significantly improved and bone regeneration accelerated.

Therefore, as a next step, our aim was to identify biomarkers, which would enable immediate identification of ASCs with enhanced bone differential potential. Thus, the time-consuming *in vitro* culturing (with all the physiological changes related with the *in vitro* culture) could be avoided and treatment could be instantaneously accomplished. Therefore, changes of expression levels of selected markers were monitored over four days of osteogenic differentiation. The MSC marker CD73 seemed to be suitable for distinguishing between good and bad lines, as its median expression value was generally remarkably lower in the good and intermediate lines in comparison to the bad lines (Fig. 16B). Another interesting marker is AP, which showed a continuous increase in the good and intermediate lines compared to the bad lines, where the abundance stayed steadily on a low level (Fig. 16A). This data again confirmed the dissimilarity between good and bad osteogenic differentiating ASC lines. The heterogeneity, which could already be seen in the undifferentiated cells at day zero, was in fact also reflected in the differentiation process. The classical MSC marker CD105 was also investigated over the time of osteogenic differentiation. In this marker, abundances did not differ in such a clearly manner than in the other two scrutinized markers CD73 and AP (Fig. 16C). Therefore, this marker would be an unsuitable marker for detection of the right set of cells.

With this preliminary staged data, even with an antibody panel containing only a limited amount of markers, differences between the ASC lines were still noticeable. Notwithstanding, a further expansion of the antibody panel with more markers for undifferentiated, as well as for cells differentiating into osteoblasts is required. With this presented data, one can clearly see that the ASC population is more complex than initially assumed. With the novel technology of CyTOF, it is possible to expand the antibody panel to a large extent. A further approach would be to isolate the specific population of cells (CD73 low and AP high) and to investigate only these specific subpopulations.

It would also be interesting to implement markers in the antibody panel for the other two mesenchymal lineages, fat and cartilage, and perform a similar analysis with mass cytometry as for the osteogenic differentiation. Exploring the same population, which was identified having enhanced osteogenic potential would be of great interest as these cells might be capable of differentiating into the other two lineages. Another more likely hypothesis would be that different subpopulations have a specific lineage propensity.

In conclusion, the results presented above, even though still on a preliminary stage, project a new vision for medical applications of ASCs. In order to achieve the possibility to directly implant the cells of interest for medical treatment, it is compulsory to develop transplantation protocols compatible with the clinics. In order to avoid *in vitro* expansion, cell sorting with specific markers (CD73 low and AP high) for enrichment of the right cells would be an interesting strategy. This procedure could be performed in parallel to the surgery of the fracture, and therefore, a second surgery as currently needed in the standard treatment of critical size bone defects would not be necessary. With this, quality of fracture repair and their subsequent clinical outcome could be ameliorated significantly and be taken on whole new level. The identified subpopulation with a higher abundance in the good osteogenic differentiating ASC lines represents a very promising approach for tissue engineering with ASCs in orthopaedic surgery.

5.2 Outlook

For this Doctoral Thesis, CyTOF analysis of ASCs was carried out with a relatively small antibody panel including only positive and negative stem cell markers as well as two osteogenic markers. Based on the data obtained, the composition of subpopulations in ASCs seems to be more complex than initially presumed. Therefore, the analysis procedure needs optimization in order to better understand the ASC composition of subpopulations. Following investigations need to be carried out for further dissection of the heterogeneity of ASCs:

- Expansion of the established antibody panel for mass cytometry. Inclusion of more markers not only for osteogenic, but also for adipogenic and chondrogenic differentiation. A new antibody of interest requires conjugation to an appropriate heavy metal and titration on both negative and positive control cells.
- Identification of new markers through transcriptomic analysis.
- In case of unavailability of specific antibodies, mRNAs can be conjugated to heavy metals. This novel approach enables specific selection of mRNAs against a markers of interest [49].
- Investigation of osteogenic differentiation with mass cytometry over a longer period of time than four days. Due to the increasing calcium deposition, trypsinisation of the differentiating cells became more challenging the longer the differentiation was carried out. A recently developed approach named imaging mass cytometry could be a possible solution for this issue [50]. With this method, osteogenic differentiating cells can be left in their cell culture dishes for analysis and therefore be differentiated for a longer period of time.
- In order to obtain an exhaustive informative panel of the 20 analysed ASC lines, it would be particularly interesting to perform a CyTOF analysis with these cell lines differentiating into adipocytes and chondroblasts in a similar way than described for the osteogenic differentiation in this Doctoral Thesis.

- The ultimate aim of the whole project would be to isolate the subpopulations with a higher osteogenic differentiation ability and their evaluation on a murine femur fracture model.
- Another interesting research topic would be the comparison of ASCs extracted not only from healthy patients, but also from patients suffering from osteoporosis.

References

[1] U. Kini and B. Nandeesh, *Physiology of Bone Formation, Remodeling, and Metabolism*. Springer-Verlag Berlin Heidelberg, 2012.

[2] M. Rauner, N. Stein, and L. C. Hofbauer, *Basics of Bone Biology*, pp. 1–26. Vienna: Springer Vienna, 2012.

[3] G. J. Tortora and B. Derrickson, *Essentials of a Anatomy and Physiology*. John Wiley & Sons, 2012.

[4] A. Oryan, S. Alidadi, A. Moshiri, and N. Maffulli, "Bone regenerative medicine: classic options, novel strategies, and future directions," *Journal of orthopaedic surgery and research*, vol. 9, no. 1, p. 1, 2014.

[5] B. J. Slater, M. D. Kwan, D. M. Gupta, N. J. Panetta, and M. T. Longaker, "Mesenchymal cells for skeletal tissue engineering," *Expert opinion on biological therapy*, vol. 8, no. 7, pp. 885–893, 2008.

[6] P. P. Spicer, J. D. Kretlow, S. Young, J. A. Jansen, F. K. Kasper, and A. G. Mikos, "Evaluation of bone regeneration using the rat critical size calvarial defect," *Nature protocols*, vol. 7, no. 10, pp. 1918–1929, 2012. Definition critical sized bone defect.

[7] H. Petite, V. Viateau, W. Bensaid, A. Meunier, C. de Pollak, M. Bourguignon, K. Oudina, L. Sedel, and G. Guillemin, "Tissue-engineered bone regeneration," *Nature biotechnology*, vol. 18, no. 9, pp. 959–963, 2000.

[8] I. Ullah, R. B. Subbarao, and G. J. Rho, "Human mesenchymal stem cells-current trends and future prospective," *Bioscience reports*, vol. 35, no. 2, p. e00191, 2015.

[9] M. Dominici, K. L. Blanc, I. Mueller, I. Slaper-Cortenbach, F. Marini, D. Krause, R. Deans, A. Keating, D. Prockop, and E. Horwitz, "Minimal criteria for defining multipotent mesenchymal stromal cells. the international society for cellular therapy position statement," *Cytotherapy*, vol. 8, no. 4, pp. 315 – 317, 2006.

[10] A. Friedenstein, R. Chailakhjan, and K. Lalykina, "The development of fibroblast colonies in monolayer cultures of guinea-pig bone marrow and spleen cells," *Cell Proliferation*, vol. 3, no. 4, pp. 393–403, 1970.

[11] W. Wagner, F. Wein, A. Seckinger, M. Frankhauser, U. Wirkner, U. Krause, J. Blake, C. Schwager, V. Eckstein, W. Ansorge, *et al.*, "Comparative characteristics of mesenchymal stem cells from human bone marrow, adipose tissue, and umbilical cord blood," *Experimental hematology*, vol. 33, no. 11, pp. 1402–1416, 2005.

[12] T. Morito, T. Muneta, K. Hara, Y.-J. Ju, T. Mochizuki, H. Makino, A. Umezawa, and I. Sekiya, "Synovial fluid-derived mesenchymal stem cells increase after intra-articular ligament injury in humans," *Rheumatology*, vol. 47, no. 8, pp. 1137–1143, 2008.

[13] A. J. Katz, A. Tholpady, S. S. Tholpady, H. Shang, and R. C. Ogle, "Cell surface and transcriptional characterization of human adipose-derived adherent stromal (hadas) cells," *Stem cells*, vol. 23, no. 3, pp. 412–423, 2005.

[14] S. E. Haynesworth, J. Goshima, V. M. Goldberg, and A. I. Caplan, "Characterization of cells with osteogenic potential from human marrow," *Bone*, vol. 13, no. 1, pp. 81–88, 1992.

[15] J. U. Yoo, T. S. Barthel, K. Nishimura, L. Solchaga, A. I. Caplan, V. M. Goldberg, and B. Johnstone, "The chondrogenic potential of human bone-marrow-derived mesenchymal progenitor cells," *J Bone Joint Surg Am*, vol. 80, no. 12, pp. 1745–57, 1998.

[16] J. E. Dennis, A. Merriam, A. Awadallah, J. U. Yoo, B. Johnstone, and A. I. Caplan, "A quadripotential mesenchymal progenitor cell isolated from the marrow of an adult mouse," *Journal of Bone and Mineral Research*, vol. 14, no. 5, pp. 700–709, 1999.

[17] H. Nakagawa, S. Akita, M. Fukui, T. Fujii, and K. Akino, "Human mesenchymal stem cells successfully improve skin-substitute wound healing," *British Journal of Dermatology*, vol. 153, no. 1, pp. 29–36, 2005.

[18] G. C. Kopen, D. J. Prockop, and D. G. Phinney, "Marrow stromal cells migrate throughout forebrain and cerebellum, and they differentiate into astrocytes after injection into neonatal mouse brains," *Proceedings of the National Academy of Sciences*, vol. 96, no. 19, pp. 10711–10716, 1999.

[19] R. S. Tuan, G. Boland, and R. Tuli, "Adult mesenchymal stem cells and cell-based tissue engineering," *Arthritis Res Ther*, vol. 5, no. 1, p. 1, 2002.

[20] E. Montelatici, B. Baluce, E. Ragni, C. Lavazza, V. Parazzi, R. Mazzola, G. Cantarella, M. Brambilla, R. Giordano, and L. Lazzari, "Defining the identity of human adipose-derived mesenchymal stem cells," *Biochemistry and Cell Biology*, vol. 93, no. 1, pp. 74–82, 2014.

[21] R. Hass, C. Kasper, S. Böhm, and R. Jacobs, "Different populations and sources of human mesenchymal stem cells (msc): a comparison of adult and neonatal tissue-derived msc," *Cell Communication and Signaling*, vol. 9, no. 1, p. 1, 2011.

[22] J. Kobolak, A. Dinnyes, A. Memic, A. Khademhosseini, and A. Mobasheri, "Mesenchymal stem cells: Identification, phenotypic characterization, biological properties and potential for regenerative medicine through biomaterial micro-engineering of their niche," *Methods*, vol. 99, pp. 62–68, 2016.

[23] M. Mo, S. Wang, Y. Zhou, H. Li, and Y. Wu, "Mesenchymal stem cell subpopulations: phenotype, property and therapeutic potential," *Cellular and Molecular Life Sciences*, pp. 1–11, 2016.

[24] R. Hass, C. Kasper, S. Böhm, and R. Jacobs, "Different populations and sources of human mesenchymal stem cells (msc): a comparison of adult and neonatal tissue-derived msc," *Cell Communication and Signaling*, vol. 9, no. 1, p. 1, 2011.

[25] S. Gao, M. Calcagni, M. Welti, S. Hemmi, N. Hild, W. J. Stark, G. M. Bürgisser, G. A. Wanner, P. Cinelli, and J. Buschmann, "Proliferation of asc-derived endothelial cells in a 3d electrospun mesh: Impact of bone-biomimetic nanocomposite and co-culture with asc-derived osteoblasts," *Injury*, vol. 45, no. 6, pp. 974–980, 2014.

[26] A. Sorrentino, M. Ferracin, G. Castelli, M. Biffoni, G. Tomaselli, M. Baiocchi, A. Fatica, M. Negrini, C. Peschle, and M. Valtieri, "Isolation and characterization of cd146+ multipotent mesenchymal stromal cells," *Experimental hematology*, vol. 36, no. 8, pp. 1035–1046, 2008.

[27] K. C. Russell, H. A. Tucker, B. A. Bunnell, M. Andreeff, W. Schober, A. S. Gaynor, K. L. Strickler, S. Lin, M. R. Lacey, and K. C. O'Connor, "Cell-surface expression of neuron-glial antigen 2 (ng2) and melanoma cell adhesion molecule (cd146) in heterogeneous cultures of marrow-derived mesenchymal stem cells," *Tissue engineering Part A*, vol. 19, no. 19-20, pp. 2253–2266, 2013.

[28] S. Gronthos, D. M. Franklin, H. A. Leddy, P. G. Robey, R. W. Storms, and J. M. Gimble, "Surface protein characterization of human adipose tissue-derived stromal cells," *Journal of cellular physiology*, vol. 189, no. 1, pp. 54–63, 2001.

[29] A. F. Nassar, H. Ogura, and A. V. Wisnewski, "Impact of recent innovations in the use of mass cytometry in support of drug development," *Drug discovery today*, vol. 20, no. 10, pp. 1169–1175, 2015.

[30] D. A. De Ugarte, Z. Alfonso, P. A. Zuk, A. Elbarbary, M. Zhu, P. Ashjian, P. Benhaim, M. H. Hedrick, and J. K. Fraser, "Differential expression of stem cell mobilization-associated molecules on multi-lineage cells from adipose tissue and bone marrow," *Immunology letters*, vol. 89, no. 2, pp. 267–270, 2003.

[31] P. Psaltis, S. Paton, F. See, A. Arthur, S. Martin, S. Itescu, S. Worthley, S. Gronthos, and A. Zannettino, "Enrichment for stro-1 expression enhances the cardiovascular paracrine activity of human bone marrow-derived mesenchymal cell populations," *Journal of cellular physiology*, vol. 223, no. 2, pp. 530–540, 2010.

[32] H. Ning, G. Lin, T. F. Lue, and C.-S. Lin, "Mesenchymal stem cell marker stro-1 is a 75kd endothelial antigen," *Biochemical and biophysical research communications*, vol. 413, no. 2, pp. 353–357, 2011.

[33] N. Quirici, C. Scavullo, L. de Girolamo, S. Lopa, E. Arrigoni, G. L. Deliliers, and A. T. Brini, "Anti-l-ngfr and-cd34 monoclonal antibodies identify multipotent mesenchymal stem cells in human adipose tissue," *Stem cells and development*, vol. 19, no. 6, pp. 915–925, 2009.

[34] S. S. Kerpedjieva, D. S. Kim, D. J. Barbeau, and K. Tamama, "Egfr ligands drive multipotential stromal cells to produce multiple growth factors and cytokines via early growth response-1," *Stem cells and development*, vol. 21, no. 13, pp. 2541–2551, 2012.

[35] R. M. Farahani and M. Xaymardan, "Platelet-derived growth factor receptor alpha as a marker of mesenchymal stem cells in development and stem cell biology," *Stem cells international*, vol. 2015, 2015.

[36] I. Albeniz, L. Türker-Şener, A. Baş, İ. Kalelioğlu, and R. Nurten, "Isolation of hematopoietic stem cells and the effect of cd38 expression during the early erythroid progenitor cell development process," *Oncology letters*, vol. 3, no. 1, pp. 55–60, 2012.

[37] F. Mair, F. J. Hartmann, D. Mrdjen, V. Tosevski, C. Krieg, and B. Becher, "The end of gating? an introduction to automated analysis of high dimensional cytometry data," *European journal of immunology*, vol. 46, no. 1, pp. 34–43, 2016.

[38] S. Van Gassen, B. Callebaut, M. J. Van Helden, B. N. Lambrecht, P. Demeester, T. Dhaene, and Y. Saeys, "Flowsom: Using self-organizing maps for visualization and interpretation of cytometry data," *Cytometry Part A*, vol. 87, no. 7, pp. 636–645, 2015.

[39] E. Arvaniti and M. Claassen, "Sensitive detection of rare disease-associated cell subsets via representation learning," *Nature communications*, vol. 8, p. 14825, 2017.

[40] A. Eichrodt, "Comprehensive mass cytometry analysis of human adipose-derived stem cells during osteogenic differentiation," Master's thesis, Departement of Trauma Surgery, University Hospital of Zurich, 2017.

[41] J. Buschmann, S. Gao, L. Härter, S. Hemmi, M. Welti, C. M. Werner, M. Calcagni, P. Cinelli, and G. A. Wanner, "Yield and proliferation rate of adipose-derived stromal cells as a function of age, body mass index and harvest siteincreasing the yield by use of adherent and supernatant fractions?," *Cytotherapy*, vol. 15, no. 9, pp. 1098–1105, 2013.

[42] Qiagen, *Critical Factors for Successful Real-Time PCR*, 2010.

[43] D. Canepa, "Identification of adipose derived stem cell subpopulations for bone regeneration," Master's thesis, Departement of Trauma Surgery, University Hospital of Zurich, 2016.

[44] S. Post, B. Abdallah, J. Bentzon, and M. Kassem, "Demonstration of the presence of independent pre-osteoblastic and pre-adipocytic cell populations in bone marrow-derived mesenchymal stem cells," *Bone*, vol. 43, no. 1, pp. 32–39, 2008.

[45] S. A. Kuznetsov, P. H. Krebsbach, K. Satomura, J. Kerr, M. Riminucci, D. Benayahu, and P. G. Robey, "Single-colony derived strains of human marrow stromal fibroblasts form bone after transplantation in vivo," *Journal of bone and mineral research*, vol. 12, no. 9, pp. 1335–1347, 1997.

[46] M. A. König, D. D. Canepa, D. Cadosch, E. Casanova, M. Heinzelmann, D. Rittirsch, M. Plecko, S. Hemmi, H.-P. Simmen, P. Cinelli, *et al.*, "Direct transplantation of native pericytes from adipose tissue: A new perspective to stimulate healing in critical size bone defects," *Cytotherapy*, vol. 18, no. 1, pp. 41–52, 2016.

[47] S. C. Bendall, E. F. Simonds, P. Qiu, D. A. El-ad, P. O. Krutzik, R. Finck, R. V. Bruggner, R. Melamed, A. Trejo, O. I. Ornatsky, *et al.*, "Single-cell mass cytometry of differential immune and drug responses across a human hematopoietic continuum," *Science*, vol. 332, no. 6030, pp. 687–696, 2011.

[48] R. V. Bruggner, B. Bodenmiller, D. L. Dill, R. J. Tibshirani, and G. P. Nolan, "Automated identification of stratifying signatures in cellular subpopulations," *Proceedings of the National Academy of Sciences*, vol. 111, no. 26, pp. E2770–E2777, 2014.

[49] A. P. Frei, F.-A. Bava, E. R. Zunder, E. W. Hsieh, S.-Y. Chen, G. P. Nolan, and P. F. Gherardini, "Highly multiplexed simultaneous detection of rnas and proteins in single cells," *Nature methods*, 2016.

[50] C. Giesen, H. A. Wang, D. Schapiro, N. Zivanovic, A. Jacobs, B. Hattendorf, P. J. Schüffler, D. Grolimund, J. M. Buhmann, S. Brandt, *et al.*, "Highly multiplexed imaging of tumor tissues with subcellular resolution by mass cytometry," *Nature methods*, vol. 11, no. 4, pp. 417–422, 2014.

Acknowledgements

Firstly, I would like to express my sincere gratitude to my main advisor PD Dr. Paolo Cinelli for giving me the opportunity to carry out my Doctoral Thesis in his research group, for his valuable guidance, and for enlightening discussions.

I am profoundly grateful to my second advisor Dr. Elisa Zimmermann, who provided me with continuous support and great advice.

My sincere thanks go to Eirini Arvaniti for her help with our mass cytometry data analysis. Furthermore, special thanks go to the people from the mass cytometry facility of the University of Zurich, especially Dr. Vinko Tosevski, for helping to conduct the experiments.

Moreover, I would like to thank the team from the Cinellis laboratory for their support: Daisy Canepa, Sonja Märsmann, Sonja Hemmi, and Benjamin Eggerschwiler.

Last but not least, I would like to thank Damian Steiger and my parents Jacqueline and Matthias Eichrodt for supporting me to achieve a doctoral's degree.

Curriculum vitae

Vorname Name	**Anna Mirjam Eichrodt**
Geburtsdatum	03.10.1990
Geburtsort	Scherzingen
Nationalität	Schweiz
Heimatort	Basel BS

08/1997 - 07/2006	**Primar-, und Sekundarschule**, Schulhaus Gelbhausgarten, Schaffhausen, Schweiz
08/07/2010	**Matura**, Kantonsschule Schaffhausen, Schweiz

09/2011 - 06/2012	**Studium Pflege**, Zürcher Hochschule für Angewandte Wissenschaften, Winterthur, Schweiz
09/2012 - 06/2017	**Studium Veterinärmedizin**, Universität Zürich, Schweiz
29/12/2017	**Abschlussprüfung vet.med.**, Universität Zürich, Schweiz

01/2018 - 01/2019	**Anfertigung der Dissertation** unter Leitung von PD Dr. Paolo Cinelli an der Klinik für Traumatologie des Universitätsspitals Zürich Direktor: Prof. Dr. med. Hans-Christoph Pape

04/2018 - heute	**Assistenztierärztin** im Internship, Ennetseeklinik für Kleintiere AG, Hühnenberg, Schweiz